## scientific reports



### **OPEN**

# An epigenetic memory at the CYP1A gene in cancer-resistant, pollution-adapted killifish

Samantha Carrothers<sup>1</sup>, Rafael Trevisan<sup>2,3</sup>, Nishad Jayasundara<sup>2</sup>, Nicole Pelletier<sup>1</sup>, Emma Weeks<sup>1</sup>, Joel N. Meyer<sup>2</sup>, Richard Di Giulio<sup>2</sup> & Caren Weinhouse<sup>1⊠</sup>

Human exposure to polycyclic aromatic hydrocarbons (PAH) is a significant public health problem that will worsen with a warming climate and increased large-scale wildfires. Here, we characterize an epigenetic memory at the *cytochrome P450 1 A* (*CYP1A*) gene in wild *Fundulus heteroclitus* that have adapted to chronic, extreme PAH pollution. In wild-type fish, *CYP1A* is highly induced by PAH. In PAH-tolerant fish, *CYP1A* induction is blunted. Since CYP1A metabolically activates PAH, this memory protects these fish from PAH-mediated cancer. However, PAH-tolerant fish reared in clean water recover *CYP1A* inducibility, indicating a non-genetic effect. We observed epigenetic control of this reversible memory of generational PAH stress in F<sub>1</sub> PAH-tolerant embryos. We detected a bivalent domain in the *CYP1A* promoter enhancer comprising both activating and repressive histone post-translational modifications. Activating modifications, relative to repressive ones, showed greater increases in response to PAH in sensitive embryos, relative to tolerant, consistent with greater gene activation. PAH-tolerant adult fish showed persistent induction of *CYP1A* long after exposure cessation, which is consistent with defective *CYP1A* shutoff. These results indicate that PAH-tolerant fish have epigenetic protection against PAH-induced cancer in early life that degrades in response to continuous gene activation.

**Keywords** Epigenetics, Polycyclic aromatic hydrocarbons, Environmental plasticity, Fundulus heteroclitus

Human exposure to polycyclic aromatic hydrocarbons (PAH) is a significant and growing public health problem<sup>1</sup>. PAH are byproducts of organic combustion that are present in high levels in cigarette smoke, coal-fired power plant emissions, vehicular exhaust, and wildfire smoke<sup>1–5</sup>. Wildfire smoke is highly mutagenic; this mutagenicity is strongly correlated with PAH content in both particulate and gas phases<sup>6</sup>. Large-scale wildfires lead to high-dose PAH exposures to human populations<sup>7</sup>. These exposure events are increasing as the climate warms; the United Nations Environment Programme predicts a global increase in extreme fires of 14% by 2030, 30% by 2050, and 50% by the end of the century<sup>7</sup>.

Sustained or extreme exposure to certain PAH causes lung cancer in humans  $^{2,4-6,8-10}$  and environmental PAH exposures are responsible for most lung cancer cases worldwide  $^{11,12}$ . A recent study in The Lancet Global Health labeled lung cancer the leading contributor to preventable death in high income countries  $^{11,12}$ . In addition, lung cancer is a common disease with poor outcomes. Lung cancer is the most common cancer (nearly 2.5 million cases per year, as of  $2020)^{13-15}$  and the leading cause of cancer deaths globally (> 1.8 million deaths in  $2020)^{13-15}$ .

Genotoxic PAH cause cancer by increasing the frequency of DNA mutations<sup>1</sup>. These PAH do not cause mutations in their parent forms; parent PAH are pro-carcinogens that are transformed into mutagenic metabolites when bioactivated by metabolic enzymes<sup>1</sup>. In mammals, the primary enzyme that bioactivates PAH is cytochrome P4501A1 (CYP1A1)<sup>16–19</sup>. CYP1A1 is a monooxygenase that adds a reactive hydroxyl group or epoxide to PAH<sup>16–19</sup>. When this hydroxyl group reacts further with a glutathione or glucuronide molecule, the resulting conjugated compound is rendered transportable out of the cell for excretion from the body<sup>16,17</sup>. However, reactive PAH metabolites can also form DNA adducts which, if unrepaired, can lead to DNA mutations<sup>16–19</sup>. High mutation burdens increase the probability of cancer driver mutations that can transform healthy cells into cancerous ones<sup>16,17</sup>. As a result, CYP1A1 activity is both required for PAH clearance and responsible for their carcinogenicity<sup>16,17</sup>. *CYP1A1* gene expression is substantially induced in the presence of PAH through ligand-dependent activation of the aryl hydrocarbon receptor (AHR), speeding xenobiotic clearance<sup>16,17,20,21</sup>. Therefore,

<sup>1</sup>Oregon Institute of Occupational Health Sciences, Oregon Health and Science University, 3181 SW Sam Jackson Park Road, 97239 Portland, OR, USA. <sup>2</sup>Nicholas School of the Environment, Duke University, 27701 Durham, NC, USA. <sup>3</sup>Present address: Univ Brest, Ifremer, CNRS, IRD, UMR 6539, LEMAR, Plouzané 29280, France. <sup>™</sup>email: weinhous@ohsu.edu

as the dose of PAH increases, so does the DNA mutation burden and cancer risk, due in part to proportionally greater *CYP1A1* expression<sup>22–24</sup>.

CYP1A1 induction predicts PAH-induced cancer risk. PAH exposure and cancer are strongly associated, but PAH-related cancer risk is highly variable among individuals. For example, tobacco smoking is an established risk factor for lung cancer, but there is considerable unexplained variation in risk among smokers<sup>25,26</sup>. Genetic polymorphisms in metabolic genes may explain some of this variation<sup>27–31</sup>. Individuals that carry one of four well-characterized mutations in CYP1A1 are at higher risk for lung cancer<sup>27–31</sup> and, in some ethnic groups, this risk is compounded in carriers that smoke<sup>30,32–34</sup>. These genetic variants likely confer increased cancer risk by increasing formation of mutagenic metabolites, either through increased enzymatic activity or through increasing inducibility of the CYP1A1 gene in the presence of PAH<sup>35–39</sup>. Since global lung cancer rates are likely to rise with rising wildfire smoke pollution, we hypothesize that preventing these sustained increases in CYP1A1 expression will mitigate increases in lung cancer rates.

To better understand how to prevent sustained increases in *CYP1A1* expression in human populations, we focus on a wild fish population that exhibits naturally depressed induction of this metabolic gene<sup>40–44</sup>. Specifically, we leverage a natural experiment in a population of wild mummichog (*Fundulus heteroclitus*) in the mainstem and tributaries of the Elizabeth River, Virginia<sup>45</sup>. This population of fish has shown rapid, evolutionary adaptation to extreme exposures to PAH derived from creosote<sup>45,46</sup>. The adaptive phenotype includes resistance to acute toxicity, developmental abnormalities, and liver cancer that occur in wild-type fish exposed to similar doses of PAH<sup>45,47</sup>. Notably, cancer resistance in these fish results from blunted induction by PAH of the gene encoding the fish's single *CYP1A* isoform, *cytochrome P450 1 A (CYP1A)*<sup>47</sup>. In PAH-tolerant fish, PAH exposure still triggers upregulation of *CYP1A*, but to a substantially lesser degree than in wild-type, PAH-sensitive fish<sup>40–44</sup>. This phenotype is not a result of maternal loading of PAH<sup>48</sup> nor is it due to maternal effects<sup>48</sup>. The blunted *CYP1A* response persists in first-generation embryos and larvae of wild-caught, PAH-tolerant fish bred in clean water in the laboratory<sup>41</sup>. However, gene inducibility partially recovers in first-generation adults and second-generation embryos <sup>41,44</sup>; third-generation embryos show complete recovery to wild-type levels<sup>41</sup>.

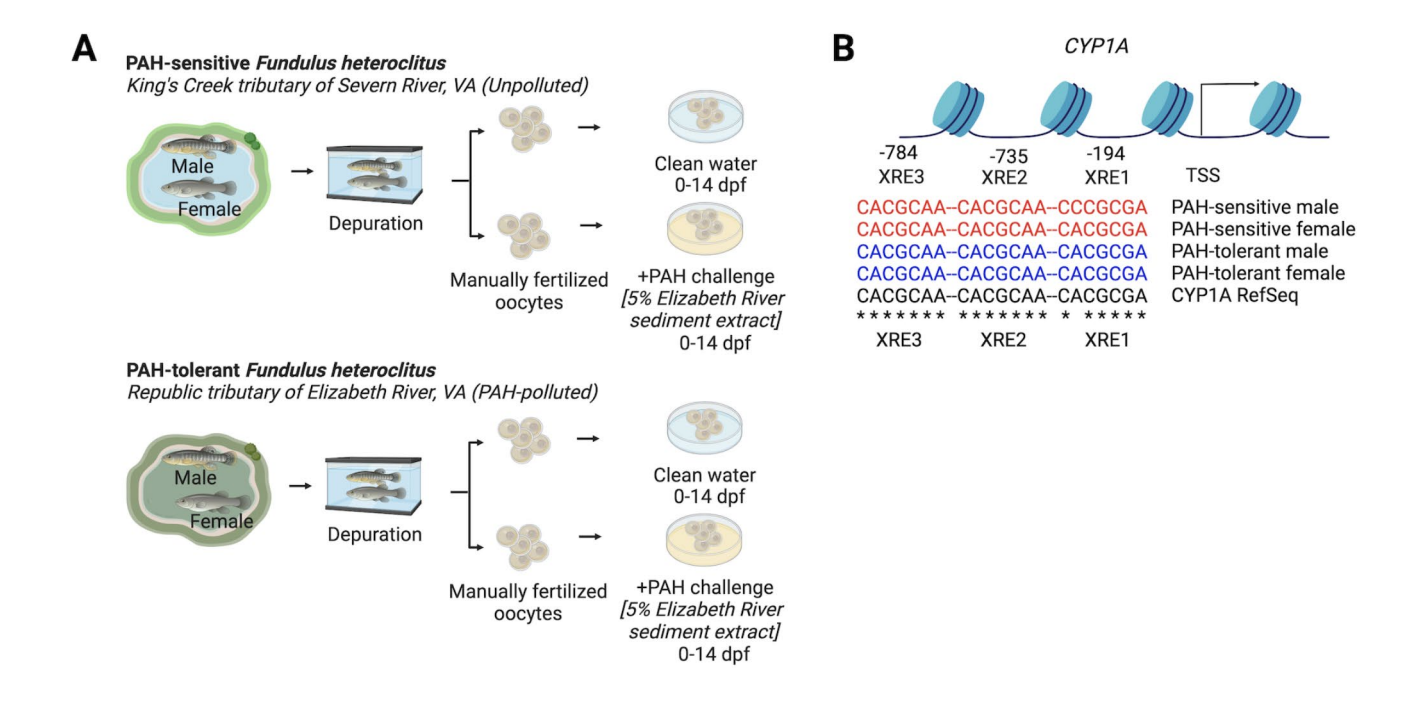
In this study, we show evidence of epigenetic control of *CYP1A* response to PAH in pollution-adapted mummichog. Our results are a critical first step in the development of preventive or therapeutic strategies for suppressing persistent induction of *CYP1A1* and reducing cancer risk in human populations with sustained, high dose PAH exposures.

#### Results

#### The CYP1A promoter-enhancer contains an environmentally-responsive bivalent domain

To explore the epigenetic memory at CYP1A, we performed experiments in wild-caught depurated adults and laboratory-bred F<sub>1</sub> embryos from both PAH-tolerant and PAH-sensitive populations of F. heteroclitus (Fig. 1A). We did not observe AHR motif sequence differences between PAH-tolerant and PAH-sensitive adult mummichog (Fig. 1B, Supporting text, Supp. Table 1, Supp. Fig. 1), which ruled out the most likely genetic explanation for reduced CYP1A inducibility in PAH-tolerant fish. Therefore, we explored potential epigenetic explanations. An epigenetic trait is a mitotically (and possibly meiotically) heritable change in gene expression or gene responsiveness that is not explained by genetic alterations<sup>49–52</sup>. Epigenetic traits involve inheritance of signaling molecules (e.g., coding or non-coding RNA, transcription factors)<sup>49,50</sup> or of structural chromatin features<sup>53-56</sup> or both. Before evaluating the CYP1A memory as an epigenetic trait, we sought to confirm prior reports of gene expression patterns at CYP1A. Using RT-qPCR, we quantified CYP1A expression in 14-day-old embryos (N = 3 pools of 10 embryos each) derived from depurated, wild-caught PAH-sensitive and PAH-tolerant adult mummichog (Fig. 1A). To quantify effect sizes in gene expression comparisons, we computed Hedge's g, which expresses effect sizes in units of standard deviation (see Methods) and is best for comparisons between groups with large variation in biological outcomes<sup>57</sup>, including gene expression patterns in these geneticallydiverse, wild fish (Fig. 1C-E). Using this approach, we observed ~4.5-fold higher basal CYP1A expression in PAH-sensitive embryos, as compared to PAH-tolerant embryos (Hedge's g: 1.68, 95% CI: -0.07, 3.32) (Supp. Fig. 2, Supp. Tables 2-3). (Hedge's g equal to or greater than 0.8 standard deviations represents a large effect, 0.4-0.6 is a moderate effect, and 0.2 is a small effect<sup>57</sup> Hedge's g point estimates are generally interpreted on this scale alone, but we add 95% confidence intervals here for completeness.) To test whether embryos from the two populations differed in their response to PAH challenge, we exposed additional embryo pools to 5% Elizabeth River sediment extract, which contains the PAH mixture present in the original contaminated site 45 (Fig. 1A). We confirmed prior reports of strong CYP1A induction in PAH-sensitive fish (>400-fold; Hedge's g: -4.57, 95% CI: -7.45, -1.27) (Fig. 1C, Supp. Fig. 2, Supp. Tables 2-3) and substantially muted CYP1A induction in PAHtolerant fish (~100-fold; Hedge's g: -8.83, 95% CI: -14.85, -2.90) (Fig. 1C, Supp. Tables 2-3). The Hedge's g metric was larger for the PAH-tolerant embryos, as compared to the PAH-sensitive, despite a much larger mean foldchange in expression in PAH-sensitive embryos, because the standard deviation in CYP1A induction was much larger in the sensitive group than in the tolerant (Fig. 1C, Supp. Fig. 2, Supp. Tables 2-3). This result indicates that epigenetic memory formation at CYP1A or genetic adaptation to PAH or a combination of both effects leads to reduced inter-individual variation in PAH response, which suggests a loss of plasticity. The Hedge's g metrics for these comparisons were both negative, since we computed differences in raw cycles-to-threshold (C(t)) values (see Methods), and C(t) is inversely correlated with gene expression. To formally quantify the difference in PAH response between populations, we computed the difference-in-difference (D-i-D), or difference in Hedge's g values; the D-i-D for [PAH-tolerant (treatment-control) – PAH-sensitive (treatment-control)] was -4.26 (95%) CI: -7.03, -1.45) (Fig. 1C, Supp. Tables 2-3), indicating an extremely large difference in CYP1A induction by PAH between the groups.

Next, we tested for the presence of similar responses at the related metabolic AHR gene targets, *CYP1B* and *CYP1C*. Prior studies showed similarly heritable but reversible resistance of these genes to induction by PAH in



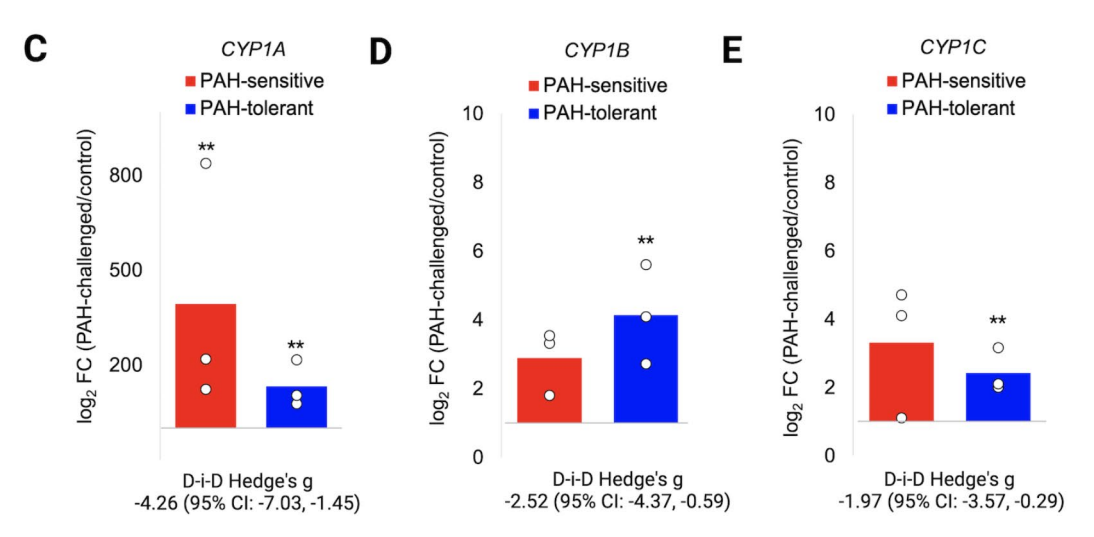


**Fig. 1.** The epigenetic memory at *CYP1A* in PAH-tolerant *Fundulus heteroclitus*. **(A)** Experimental design schematic for depuration of wild-caught fish, manual fertilization of embryos, and exposure to PAH. **(B)** Xenobiotic response elements (XREs) in the *CYP1A* proximal promoter-enhancer are conserved across four fish (one male and one female each from PAH-tolerant and PAH-sensitive populations). **(C–E)** Relative fold-change values for embryonic gene expression for three AHR target genes (*CYP1A*, *CYP1B*, and *CYP1C*). Figures show C(t) values from PAH-challenged embryo samples normalized to the average control C(t). \*\*P-value < 0.01 from independent samples t-tests comparing C(t) values from PAH-challenged embryos to control embryos within each group. Hedge's g values represent effect sizes for difference-in-difference (D-i-D) tests [PAH-tolerant (treatment-control)] – [PAH-sensitive (treatment-control)]. Hedge's g = 0.2 is a small effect, Hedge's g = 0.4–0.6 is a moderate effect, Hedge's g = or > 0.8 is a large effect. 95% confidence intervals that do not cross zero reflect *p* < 0.05. Dpf – days post-fertilization, PAH – polycyclic aromatic hydrocarbons, D-i-D – Difference-in-difference, XRE – xenobiotic response element, TSS – transcription start site.

tolerant fish<sup>44</sup>. Both *CYP1B* (PAH-sensitive: Hedge's g: -1.62, 95% CI: -3.24, 0.10; PAH-tolerant: Hedge's g: -4.15, 95% CI: -7.16, -1.10) and *CYP1C* (PAH-sensitive: Hedge's g: -1.41, 95% CI: -2.95, 0.23; PAH-tolerant: Hedge's g: -3.39, 95% CI: -5.95, -0.77) were induced by PAH in embryos, albeit to a lesser degree than *CYP1A* (Fig. 1D-E, Supp Table 2, and 3). Like *CYP1A*, both genes showed larger Hedge's g effect sizes in PAH-tolerant embryos, which suggests similarly reduced inter-individual differences in PAH response as a consequence of adaptation (*CYP1B* D-i-D -2.52, 95% CI: -4.37, -0.59; *CYP1C* D-i-D -1.97, 95% CI: -3.57, -0.29) (Supp Table 2, and 3).

CYP1C, but not CYP1B, displayed greater average fold-change response to PAH in sensitive embryos than in tolerant ones (Fig. 1D-E, Supp. Tables 2–3).

We hypothesized that these gene expression patterns resulted from epigenetic inheritance of exposureinduced changes in structural chromatin features. Structural chromatin features, including methylation of cytosine-guanine dinucleotides in DNA and post-translational modifications to histone proteins  $^{52}$ , regulate gene expression  $^{52}$  and are both environmentally responsive  $^{58}$  and inherited through cell division  $^{54-56}$ . One earlier study reported a complete absence of DNA methylation in the CYP1A promoter-enhancer in both PAH-tolerant and -sensitive fish, with or without PAH exposure<sup>59</sup>. Therefore, using chromatin immunoprecipitation (ChIP), we explored the potential roles of three histone post-translational modifications (PTMs): trimethylation of lysine 4 on histone H3 (H3K4me3), which is associated with active promoters<sup>60</sup>; monomethylation of the same lysine (H3K4me1), which marks active enhancers<sup>61</sup>; and trimethylation of lysine 27 on histone H3 (H3K27me3), which is associated with gene repression at both promoters and enhancers 62-64. We anticipated that the CYP1A promoter-enhancer in wild-type, PAH-sensitive fish would show low levels of activating histone PTMs at baseline that would increase in response to PAH challenge, and no repressive histone PTMs. In PAH-tolerant fish, we hypothesized that levels of activating histone PTMs would increase with PAH challenge, but to a lesser degree than in sensitive fish. We also anticipated that repressive histone PTMs would be newly present at the promoter to counteract strong gene induction. However, we observed a bivalent chromatin state, characterized by activating and repressive histone modifications<sup>65,66</sup>, encompassing all XREs and the TSS in both PAHsensitive and PAH-tolerant embryos (Fig. 2A-C, Supp. Fig. 3, Supp. Tables 4-8). Tolerant embryos showed lower levels of H3K4me3 and higher levels of both H3K4me1 and H3K27me3 at baseline (Supp. Figs. 3, 4 and 5, Supp. Tables 4-8). These differences in baseline histone PTMs may be due to non-genetic inheritance of parental PAH response or to unidentified genetic changes disrupting sequence specificity for histone-containing nucleosomes<sup>67</sup> or to a combination of both effects. In addition, embryos from each population displayed markedly different responses to PAH challenge (Fig. 2A-C, Supp. Fig. 3, Supp. Tables 4-8). Consistent with strong gene induction, PAH-sensitive embryos showed modest increases in average enrichment of both activating modifications at the TSS, and in H3K4me1 at XREs, combined with a decrease in repressive H3K27me3 across the promoterenhancer (Fig. 2A-C, Supp. Fig. 3, Supp. Tables 4-8). However, despite a marked increase in CYP1A expression in these embryos, most of these differences in mean histone PTM levels yielded small to moderate effect sizes in mixed models comparing exposed to control pools. This outcome likely is attributable to high inter-individual variation, including in H3K4me3 at the TSS (Hedge's g: 0.08) and at all four loci for both H3K4me1 (TSS Hedge's g: 0.34; XRE1 Hedge's g: 0.44; XRE2 Hedge's g: 0.39; XRE3 Hedge's g: 0.06) and H3K27me3 (TSS Hedge's g: -0.22; XRE1 Hedge's g: -0.22; XRE2 Hedge's g: 0.04; XRE3 Hedge's g: -0.19) (Fig. 2A-C, Supp. Fig. 3, Supp. Tables 4-8). In contrast, PAH-tolerant embryos showed a muted increase in average enrichment of H3K4me3 at the TSS and dramatic decreases in both H3K4me1 and H3K27me3 (Fig. 2A-C, Supp. Fig. 3, Supp. Tables 4-8). Following the same pattern as CYP expression data, effect sizes expressed in standard deviations were larger in tolerant embryos than in sensitive embryos for both H3K4me1 (TSS Hedge's g: -0.50; XRE1 Hedge's g: -0.63; XRE2 Hedge's g: -0.25; XRE3 Hedge's g: -0.56) and H3K27me3 (TSS Hedge's g: -1.17; XRE1 Hedge's g: -1.20; XRE2 Hedge's g: -1.36; XRE3 Hedge's g: -1.07), and accordingly smaller for H3K4me3 at the TSS (Hedge's g: 0.08). We confirmed the differences in effects between populations by computing D-i-D metrics for [PAH-tolerant (treatment-control) – PAH-sensitive (treatment-control)] (Fig. 2A-C, Supp. Tables 4-8). The pattern of activating modifications that we observed in tolerant embryos was consistent with decreased promoter and enhancer activity, which matched our observed blunted CYP1A induction. Decreased regulatory element activity may be due to reduced AHR binding or altered enhancer response to AHR binding. However, we did not have an immediate explanation for the significant decrease in H3K27me3 in tolerant embryos challenged with PAH. We reasoned that, because these modifications work together to produce a chromatin state at bivalent loci, the relative proportion of repressive to activating modifications would be more informative than enrichment of individual modifications. Therefore, we calculated the ratio of repressive to activating modifications (H3K27me3/H3K4me1 and H3K27me3/H3K4me3) (Fig. 2D-E, Supp. Fig. 4, Supp. Tables 9–10). Neither ratio differed by population at baseline (Supp. Fig. 4, Supp. Tables 9-10). In response to PAH challenge, the H3K27me3/H3K4me1 ratio showed a substantial decrease in sensitive embryos (i.e., large increases in the relative enrichment of activating modifications, as compared to repressive ones), as compared to a slight decrease in tolerant embryos (Fig. 2D, Supp. Fig. 4, Supp. Table 9). These findings agree with the blunted gene induction seen in these embryos. The H3K27me3/H3K4me3 ratio showed similar decreases in response to PAH; sensitive embryos showed greater decreases in this ratio at the TSS and its nearest XRE, XRE1, as compared to tolerant ones (Fig. 2E-F, Supp. Fig. 4, Supp. Table 10). Together, these data indicate a generationally heritable epigenetic memory of ancestral PAH exposure in a PAH-tolerant population. This memory manifests in blunted responses to PAH challenge at CYP1A, both in regulation of a promoter bivalent domain and in transcriptional output, in exposure-naïve embryos.

#### Continuous PAH exposure triggers a secondary epigenetic memory at CYP1A in adult fish

Most prior evidence of the CYP1A epigenetic memory was generated through studies of developmental toxicity of PAH and therefore focused on testing effects in exposure-naïve embryos. However, if memory formation is distinct from PAH developmental toxicity, then we would expect to see memory effects in adult animals, too. To test this hypothesis, we measured CYP1A mRNA levels in liver tissue from depurated, wild-caught adult fish from both sensitive and tolerant populations (parents of the embryos used in the prior set of experiments) (N=5 males and N=5 females per population). PAH-sensitive adults in this experiment were PAH-naïve; PAH-tolerant adults had no ongoing or residual PAH exposure but did have a long history of sustained, extreme exposure in the wild. We focused on liver tissue, since fish do not have human-equivalent lungs; fish are primarily exposed to PAH via ingestion of contaminated water and humans are primarily exposed via inhalation of contaminated air. In addition, the CYP1A memory was previously characterized in adult mummichog liver tissue  $^{41,42}$ , since

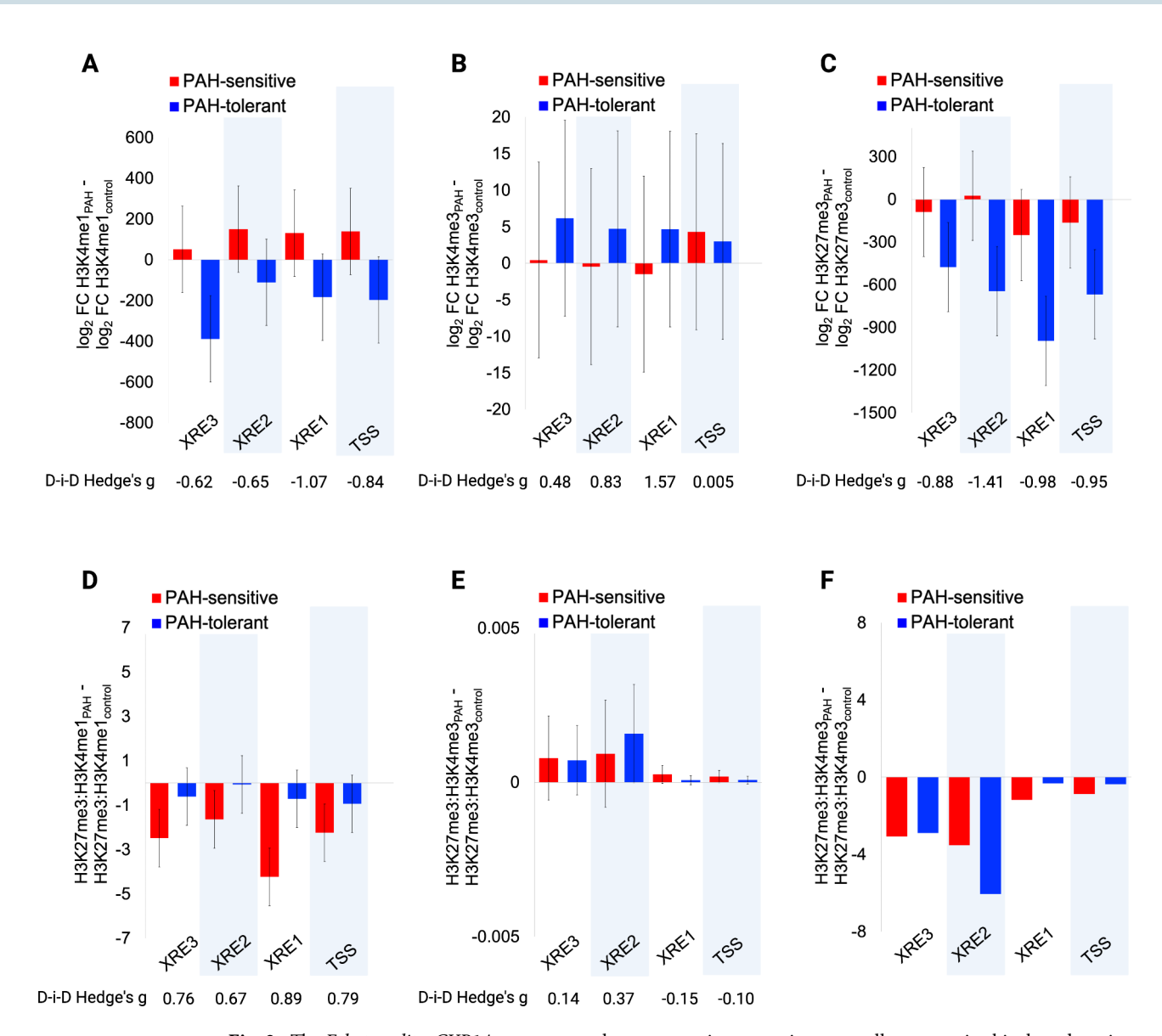


**Fig. 2.** The *F. heteroclitusCYP1A* promoter-enhancer contains an environmentally-responsive bivalent domain. (**A–C**) Mean and SEM for differences in histone PTM (H3K4me1, H3K4me3, H3K27me3) enrichment at the *CYP1A* proximal promoter-enhancer in embryos challenged with PAH (relative to control) from PAH-tolerant and PAH-sensitive populations. (**D–F**) Mean and SEM for differences in ratios of repressive/activating histone PTMs (**D**) H3K27me3/H3K4me1; (**E**) H3K27me3/H3K4me3) in embryos challenged with PAH (relative to control) from PAH-tolerant and PAH-sensitive populations. The ratio differences shown in (**E**) are inverse transformed, due to skewed data distribution. For ease of interpretation, differences in back-transformed means are shown in (**F**). Hedge's g values represent effect sizes for difference-in-difference (D-i-D) tests [PAH-tolerant (treatment-control)] – [PAH-sensitive (treatment-control)]. Hedge's g = 0.2 is a small effect, Hedge's g = 0.4 - 0.6 is a moderate effect, Hedge's g = 0.8 is a large effect. 95% confidence intervals shown in Supplemental Tables 5-8. XRE – xenobiotic response element, TSS – transcription start site.

liver is the organ with the highest concentration of CYP1A protein<sup>20</sup>. We observed higher *CYP1A* expression in PAH-tolerant adults, as compared to PAH-sensitive adults, even in the absence of PAH challenge (Hedge's g: -1.43, 95% CI: -2.37, -0.45) (Fig. 3A, Supp. Fig. 5, Supp. Tables 11–12). Notably, this effect was strongest in male fish (Hedge's g: -2.38, 95% CI: -3.94, -0.74), as compared to female fish (Hedge's g: -0.56, 95% CI: -1.69, 0.6) (D-i-D for [(PAH-tolerant males - PAH-sensitive males) – (PAH-tolerant females - PAH-sensitive females)] Hedge's g: -1.82, 95% CI: -3.0, -0.59) (Fig. 3A, Supp. Fig. 5, Supp. Tables 11–12). This result indicates a larger difference between males from the two populations than between females.

Since male fish from both populations are known to exhibit higher magnitude induction of *CYP1A* in response to PAH than female fish<sup>41,42,68</sup>, and, in our experiment, tolerant female fish did not show residual activity after exposure cessation, this result strongly suggests incomplete shutoff of the gene after exposure cessation in male fish. It is possible that this effect was partially due to higher gene expression in males in both populations. To rule this out, we tested whether *CYP1A* expression was sex-specific within populations, and if so, whether

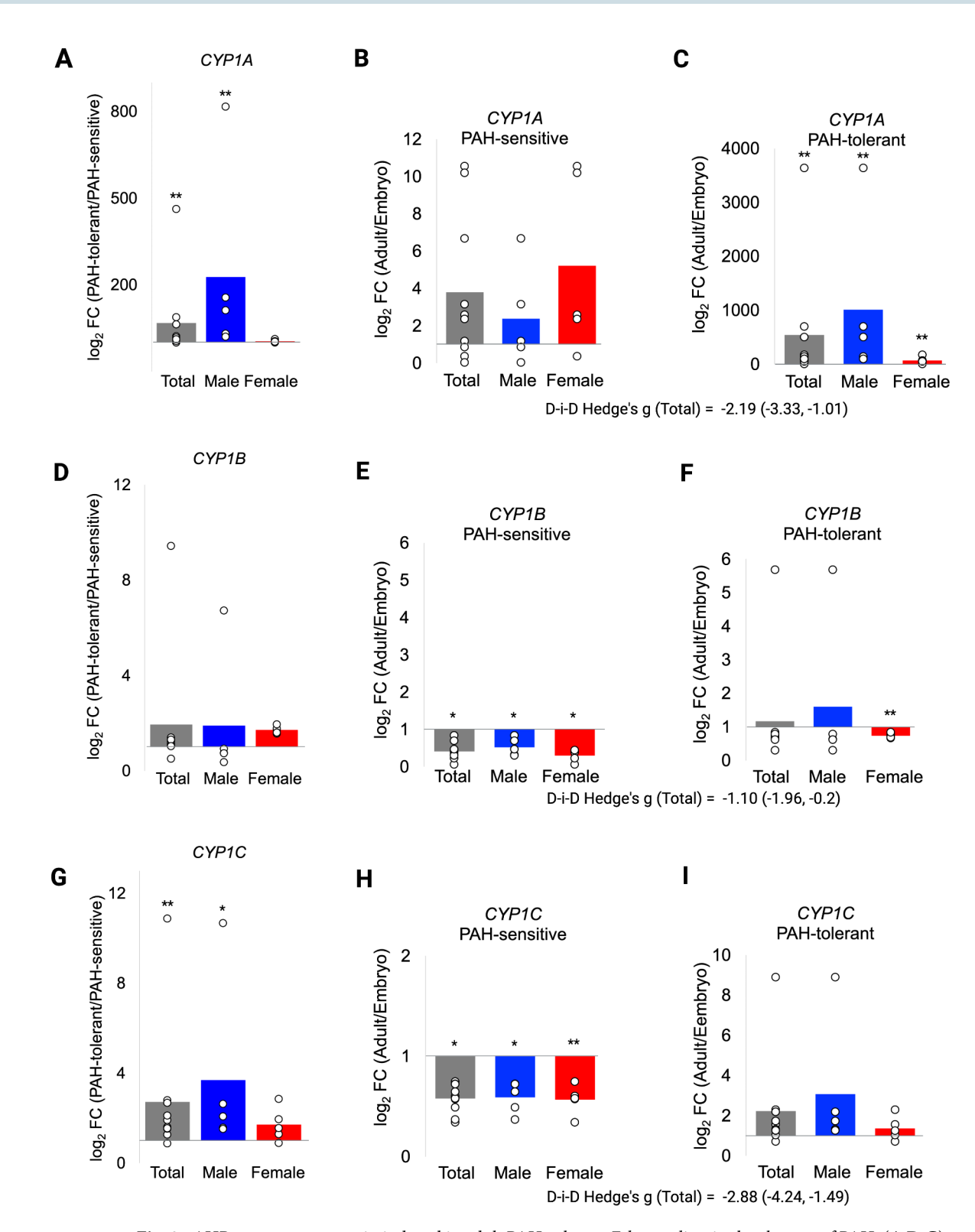


**Fig. 3.** AHR target genes remain induced in adult PAH-tolerant *F. heteroclitus* in the absence of PAH. (**A,D,G**) Relative fold-change in gene expression of the AHR target genes CYP1A (a), CYP1B (d), and CYP1C (g) in adult fish from a PAH-tolerant vs. PAH-sensitive population. (**B–C, E–F, H–I**) Relative fold-change in CYP1A (b-c), CYP1B (e-f), and CYP1C (h-i) expression in adult fish relative to embryos from the same population (PAH-sensitive or PAH-tolerant). All figures show C(t) values from adult liver tissue normalized to the average C(t) for each comparison group (PAH-sensitive adults in (**A, D, G**) and embryos in (**B–C, E–F, H–I**), separated by sex. \*\*P-value < 0.01 and \* P-value < 0.05 for independent samples t-tests of C(t) values. Hedge's P values represent effect sizes for difference-in-difference (D-i-D) tests P tests (adult-embryo)] – P the label "Total" indicates combined male and female data. Hedge's P = 0.2 is a small effect, Hedge's P = 0.4–0.6 is a moderate effect, Hedge's P = 0.8 is a large effect. 95% confidence intervals that do not cross zero reflect P < 0.05.

this sex difference was the same in both populations. We observed a moderate increase in baseline *CYP1A* expression in sensitive female fish over male fish (Hedge's g: 0.60, 95% CI: -0.57, 1.74) (Supp. Fig. 5, Supp. Tables 11–12), but a very substantial increase in residual *CYP1A* expression in tolerant male fish vs. females (Hedge's g: -1.42, 95% CI: -2.70, -0.08) (Supp. Fig. 5, Supp. Tables 11–12). We also tested whether our observation of differences in adult expression was partially due to expected changes with normal development. To evaluate this, we compared *CYP* gene expression in each group of adult fish to gene expression in the group of population-matched control embryos. *CYP1A* expression increases up to 10-fold in PAH-sensitive adult fish, as compared to embryos (Fig. 3B, Supp. Figs. 1 and 5, Supp. Table 13). In contrast, *CYP1A* expression increased ~ 1000-fold in male and ~70-fold in female PAH-tolerant adults, as compared to embryos (Fig. 3C, Supp. Figs. 1 and 5, Supp. Table 13). Taken together, our findings support the interpretation that *CYP1A* expression in PAH-tolerant male adults represents incomplete recovery from prior PAH exposure. These results suggest the formation of a secondary epigenetic memory within individual, PAH-tolerant fish that forms with sustained PAH challenge.

To further characterize this secondary epigenetic memory in adult PAH-tolerant fish, we tested two additional hypotheses. Some prior data on epigenetic memory suggests that the strength of initial gene induction predicts epigenetic memory formation<sup>69</sup>. Therefore, we asked whether sustained gene expression following exposure cessation was specific to *CYP1A*, a gene with a high induction response (>100-fold). If so, we would not see similarly sustained responses at AHR target genes *CYP1B* and *CYP1C*, both of which are induced <10-fold by PAH in exposure-naïve embryos from both populations (Fig. 1D-E). Contrary to this hypothesis, we observed similarly sustained expression for both genes in tolerant adults (Fig. 3D-I, Supp. Fig. 5, Supp. Tables 11–12).

Next, we asked whether this secondary epigenetic memory was associated with altered regulation of the promoter-enhancer bivalent domain. Bivalent domains were initially described as key regulators of developmental gene expression<sup>65,66,70-72</sup>. At most loci, bivalency resolves during lineage determination and cellular differentiation; loci that initiate transcription lose H3K27me3 and retain H3K4me3<sup>73–80</sup>, and loci that are silenced retain H3K27me3 and lose H3K4me3<sup>65</sup>. However, not all bivalent regions resolve in differentiated tissues<sup>66,81–83</sup>. To test whether the bivalent domain persists at CYP1A in adult mummichog, we measured histone PTMs in liver tissue from the same wild-caught adult male fish that showed residual CYP gene expression. We confirmed the persistence of the bivalent domain encompassing all three XREs and TSS in adult fish from both populations (Fig. 4A-C, Supp. Tables 15-17). As compared to sensitive males, tolerant male fish showed approximately equal levels of activating H3K4me1 (Supp. Table 15), moderately lower levels of activating H3K4me3 (Supp. Table 16), and moderately higher levels of repressive H3K27me3 (Supp. Table 17), none of which correlated well with the increased CYP1A expression in these males (Fig. 3A-C). In addition, the H3K27me3/H3K4me1 ratio was moderately elevated in the two XREs nearest to the TSS (Supp. Table 18), and the H3K27me3/H3K4me3 ratio was elevated across the promoter-enhancer region, particularly at the TSS (Supp. Table 19). These data indicate a relative increase in repressive signal at this bivalent domain in tolerant animals. To confirm that these results were not driven by differences in baseline histone PTMs or in changes in histone modifications with development, we compared histone PTM levels within each group of adult fish to levels in population-matched, exposure-naïve embryos and then compared developmental trajectories between populations. In agreement with the results from our initial analyses, tolerant male adults showed smaller decreases in activating PTMs and substantial increases of the repressive PTM when compared to their matched embryos, as compared to sensitive male fish (Fig. 4A-C, Supp. Fig. 6-8, Supp. Tables 20-23). Similarly, we observed increases (both in mean enrichment and in Hedge's g values that account for population variation) in both ratios in PAH-tolerant adults, as compared to PAH-sensitive ones (Fig. 5, Supp. Fig. 9-10, Supp. Tables 24-25). We speculate that this result indicates a progressive loss of regulatory control of CYP1A transcription in PAH-tolerant adults, perhaps related to the differential PAH response that we observed in matched embryos. The relative increases in the mildly repressive H3K27me3 may represent a compensatory response in tolerant fish, in an attempt to shut off the persistently induced CYP1A gene. Together, these data indicate an additional, mitotically heritable epigenetic memory of sustained PAH exposure that manifests in sustained increases in repressive: activating histone PTM ratios in the CYP1A bivalent domain and a sustained increase in expression of the CYP1A gene after cessation of PAH stimulus.

#### The human CYP1A1 promoter contains a bivalent domain and a CpG island

To evaluate the generalizability of this phenotype to human populations, we asked whether a similar bivalent domain is present at the human orthologs, CYP1A1/2 and CYP1B1. Humans have no known ortholog of CYP1C. Using publicly available Epigenome Roadmap reference datasets, we identified bivalent domains in the promoter of CYP1A1, but not CYP1A2, in human embryonic stem cells (H1 ESCs) and terminally-differentiated, karyotypically-normal lung fibroblasts (IMR90) (Supp. Fig. 11-12). These findings support a role for this bivalent domain in regulation of this gene in both embryonic and adult tissues. Because bivalent chromatin preferentially forms in DNA sequence that contains a high density of cytosine-guanine dinucleotides, or CpG islands for we tested for the presence of a CpG island at the mummichog CYP1A and the human CYP1A1. We observed two CpG islands upstream of the mummichog CYP1A, one of which overlaps the CYP1A promoter-enhancer region (Supp. Fig. 13). Similarly, we observed a CpG island upstream of the human CYP1A1 isoform, which is consistent with formation of bivalent domains at the human CYP1A(1) ortholog (Supp. Fig. 11). Therefore, human CYP1A1 contains the known structural chromatin features that characterize the CYP1A gene in mummichog, which supports the generalizability of the mummichog CYP1A memory phenotype to humans.

#### Discussion

Here, we characterize an epigenetic memory at the *CYP1A* gene that arose naturally in a wild Atlantic mummichog population as it adapted to chronic, extreme PAH pollution. In PAH-tolerant fish, *CYP1A* induction is blunted. However, tolerant fish reared in clean water in the laboratory for one generation partially recover

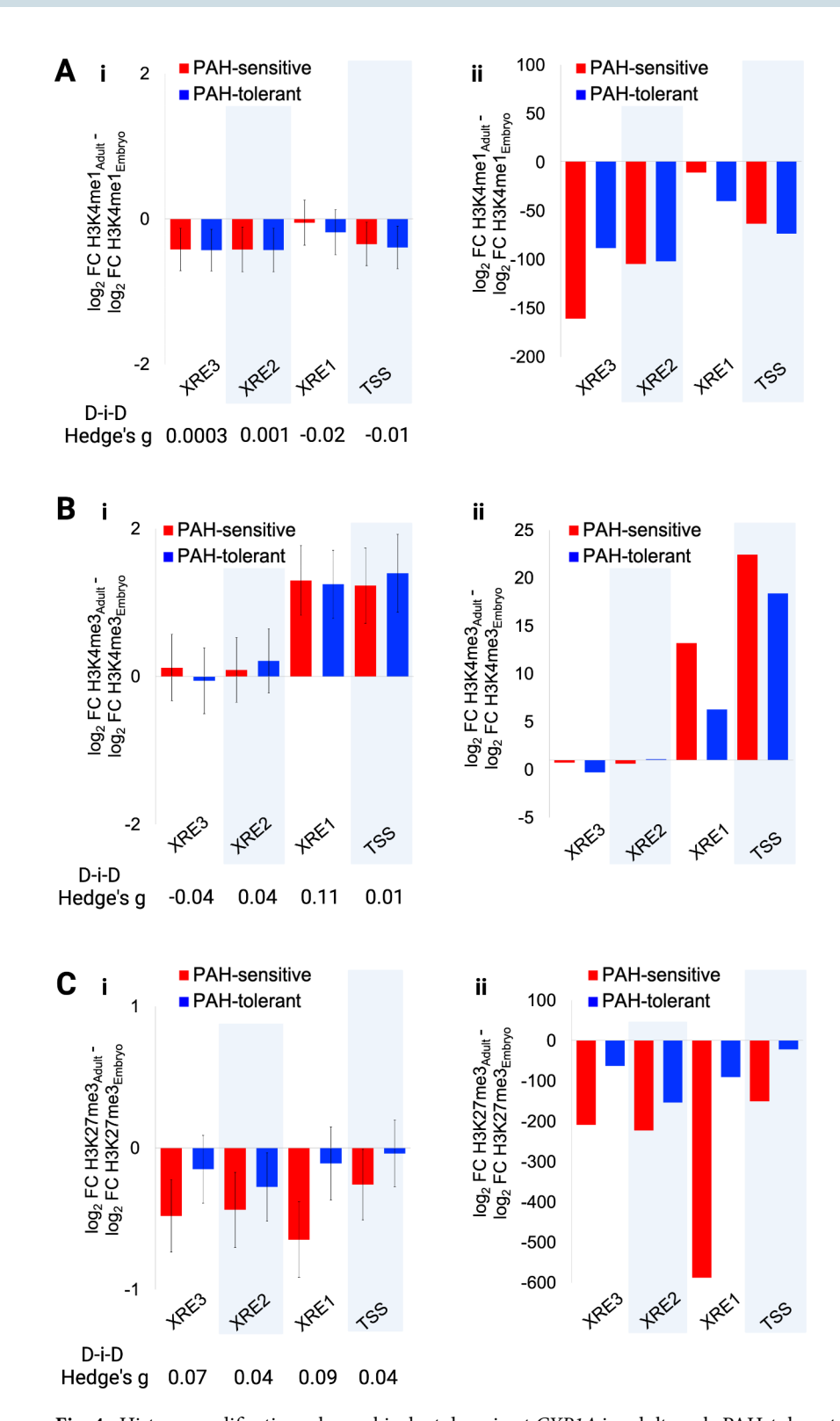


**Fig. 4.** Histone modifications show a bivalent domain at *CYP1A* in adult, male PAH-tolerant fish. ( $\mathbf{A_i}$ ,  $\mathbf{B_i}$ ,  $\mathbf{C_i}$ ) Mean and SEM for differences in inverse-transformed histone PTM H3K4me1 ( $\mathbf{A_i}$ ), H3K4me3 ( $\mathbf{B_i}$ ), and H3K27me3 ( $\mathbf{C_i}$ ) at the *CYP1A* proximal promoter-enhancer in adult fish compared to matched embryos from PAH-tolerant and PAH-sensitive populations. ( $\mathbf{A_{ii}}$ ,  $\mathbf{B_{ii}}$ ,  $\mathbf{C_{ii}}$ ) Differences in back-transformed means for H3K4me1 (Aii), H3K4me3 ( $\mathbf{B_{ii}}$ ), and H3K27me3 ( $\mathbf{C_{ii}}$ ), for ease of interpretation. Hedge's g values represent effect sizes for difference-in-difference (D-i-D) tests [PAH-tolerant (adult-embryo)] – [PAH-sensitive (adult-embryo)]. Hedge's g = 0.2 is a small effect, Hedge's g = 0.4–0.6 is a moderate effect, Hedge's g = or > 0.8 is a large effect. 95% confidence intervals shown in Supplemental Tables 9–10. XRE – xenobiotic response element, TSS – transcription start site.

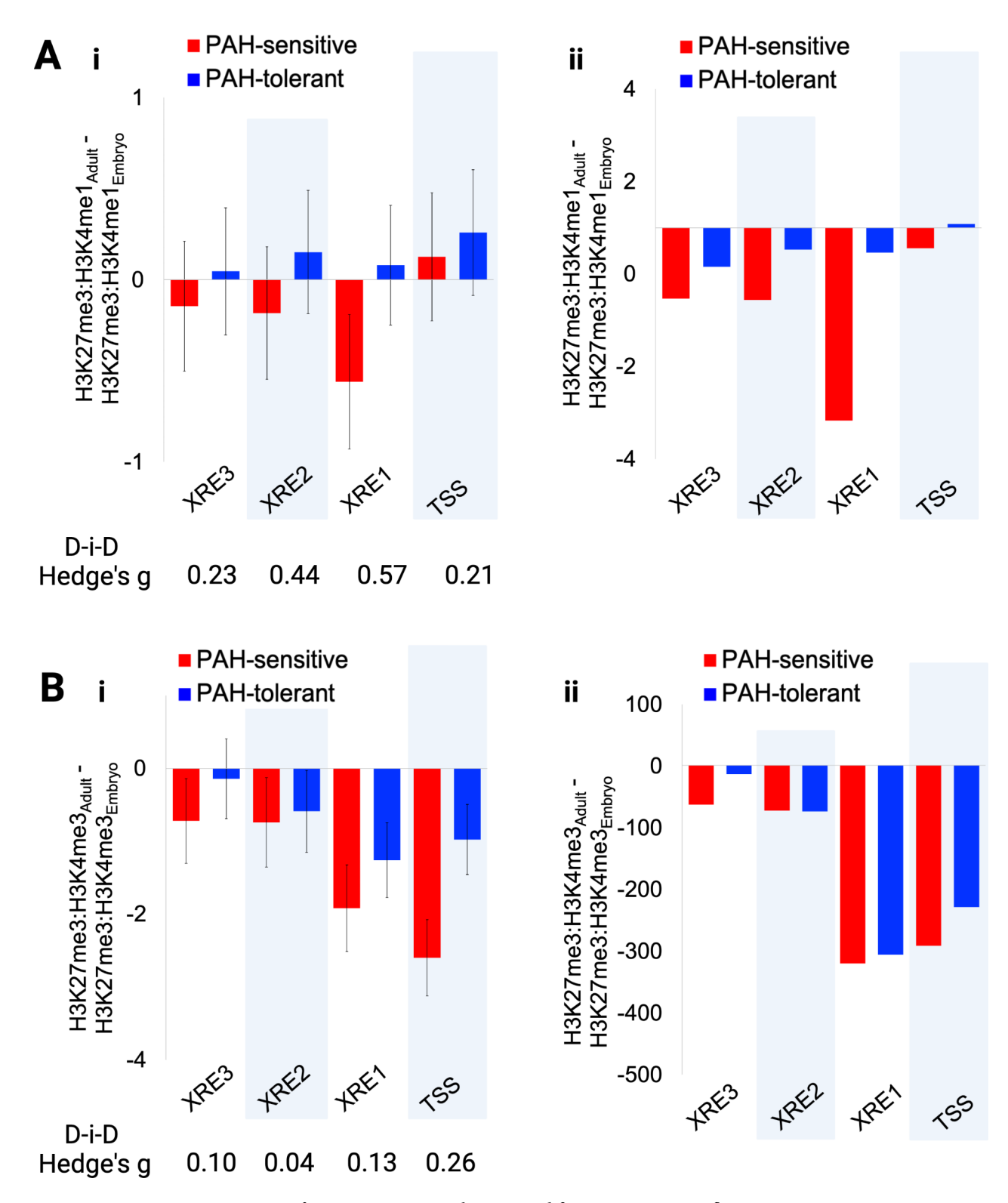


**Fig. 5.** Ratios of repressive/activating histone modifications at *CYP1A* reflect active gene expression in PAH-tolerant fish with past but no current PAH exposure. ( $\mathbf{A_i}$ ,  $\mathbf{B_i}$ ) Mean and SEM for differences in inverse transformed ratios of repressive/activating histone PTMs ((A) H3K27me3/H3K4me1; (B) H3K27me3/H3K4me3) in adult vs. embryos from both populations. ( $\mathbf{A_{ii}}$ ,  $\mathbf{B_{ii}}$ ) Differences in back-transformed means in ratios. Hedge's g values represent effect sizes for difference-in-difference (D-i-D) tests [PAH-tolerant (adult-embryo)] – [PAH-sensitive (adult-embryo)]. Hedge's g = 0.2 is a small effect, Hedge's g = 0.4–0.6 is a moderate effect, Hedge's g = 0.8 is a large effect. 95% confidence intervals shown in Supplemental Tables 24–25. XRE – xenobiotic response element, TSS – transcription start site.

CYP1A inducibility. To explore the underlying mechanism, we caught wild mummichog from PAH-tolerant and PAH-sensitive populations, manually fertilized eggs, and exposed half of the embryos in each group to 5% Elizabeth River sediment extract for 14 days post-fertilization. We identified a bivalent domain, characterized by both activating and repressive histone post-translational modifications, in the CYP1A proximal promoterenhancer in both sensitive and tolerant embryos and adults. In response to PAH, sensitive embryos showed more marked decreases in ratios of repressive/activating histone PTMs (consistent with gene activation), as compared to tolerant embryos, indicating active regulation by this domain. In addition to blunted induction of CYP1A, we observed that unexposed, PAH-tolerant adult males with a history of extreme PAH exposure showed persistent upregulation of CYP1A, which is consistent with a defect in gene recovery to baseline. Notably, PAH-sensitive fish showed greater variation than did PAH-tolerant fish in CYP1A expression and histone PTM enrichment both at baseline and in response to PAH. This result mirrors the loss of genetic diversity previously reported in PAH-tolerant fish <sup>46</sup> and suggests that genetic differences between tolerant and sensitive populations play a partial role in the observed epigenetic memory at CYP1A.

Overall, our data are consistent with two related epigenetic memories at CYP1A. The first memory is characterized by blunted PAH-triggered induction of CYP1A in PAH-tolerant embryos that correlates well with changes in histone PTMs in the promoter bivalent domain. This memory may be unique to CYP1A; alternatively, it may reflect protective epigenetic downregulation of AHR signaling that is reflected in localized chromatin responses at target genes, including CYP1A, CYP1B, and CYP1C. In the second scenario, epigenetic downregulation likely develops to protect against teratogenic effects, rather than cancer; regardless of its etiology, this memory protects against cancer. PAH-tolerant mummichog living in PAH-contaminated areas of the Elizabeth River show higher rates of cancer in liver (the primary PAH target tissue in fish), as compared to PAH-sensitive fish living in a clean environment. However, clean water-reared F, larvae of wild-caught sensitive fish exposed to a standardized dose of PAH developed more juvenile liver tumors, as compared to similarly treated tolerant F, larvae<sup>47</sup>. The second memory is characterized by persistent induction of CYP1A after exposure cessation in PAH-tolerant adult fish with a history of chronic, continuous PAH exposure, which is consistent with defective CYP1A gene shutoff and recovery to baseline. Since CYP1A expression is positively correlated with cancer risk in both mummichog and humans, these results indicate that the PAH-tolerant fish have epigenetic protection against PAH-induced cancer in early life that degrades over time in response to continuous gene activation.

These findings on naturally occurring epigenetic memories at mummichog *CYP1A* represent an important advance over existing data on experimentally-induced epigenetic memories at *CYP1A1/Cyp1a1* in mammals in response to acute exposures<sup>84–87</sup>. Four prior studies report mammalian epigenetic memories at this gene; three of the four studies show that an initial stimulus triggered sustained induction of *Cyp1a1* in exposure-naïve rodents<sup>84,85</sup> or *CYP1A1* in exposure-naïve human cells<sup>86</sup> and the fourth showed both sustained induction and superinduction on secondary challenge<sup>87</sup>. Those studies model initial responses in human populations without significant historical PAH exposures. However, few human populations today are naïve to PAH exposure, and most are likely to experience episodic, possibly chronic, exposure as wildfires increase in frequency. Therefore, PAH-tolerant mummichog represent a more informative model of human population responses. Our data suggest that chronically-exposed human populations may develop epigenetic memories that affect adult cancer risk.

Increased understanding of the epigenetic memory at mummichog *CYP1A* provides insight into approaches for protecting human health in the context of increased population exposure to PAH. Specifically, we can leverage fundamental understanding of epigenetic memory formation at *CYP1A* to develop preventive or therapeutic approaches and to protect individuals that naturally form memories from deleterious increases in baseline *CYP1A1* expression. Rodent studies show that CYP1A1 is druggable with small molecule inhibitors<sup>88–91</sup>, including dietary polyphenols<sup>88–91</sup>, or with synthetic substrates that are converted to protective molecules (e.g., compounds that are cytotoxic to cancer cells) at a higher rate when *CYP1A1* is induced<sup>92–100</sup>. If these compounds are proven safe and effective in human populations, then preventive or therapeutic treatment with these compounds may protect individuals that are either at high cancer risk from wildfire smoke exposure or at high risk of exacerbation of pre-existing cancer.

#### Materials and methods Fish collection

We caught wild mummichog from a PAH-tolerant population from the site of former creosote wood treatment facility (Republic Creosoting) in the southern of the Elizabeth River in Virginia (36° 79' 31.0" N, 76° 29' 41.3" W) and from a PAH-sensitive reference population from King's Creek, a relatively uncontaminated tributary of the Severn River in Virginia (37° 30' 47.6" N, 76° 41' 63.9" W). We depurated fish for at least 4 weeks prior to breeding in flow-through systems comprising a series of 30-40 L tanks containing 20% artificial sea water (ASW, Instant Ocean, Foster & Smith, Rhinelander, WI, USA). We maintained adult fish at 23-25 °C on a 14:10 light: dark cycle and ad libitum pelleted feed (Aquamax Fingerling Starter 300, PMI Nutrition International LLC, Brentwood, MO, USA). We obtained eggs from each population by manual spawning of females and fertilized eggs in vitro with expressed sperm from males in a beaker containing ASW. Embryos were held for one hour after spawning to allow for fertilization, then washed briefly with 0.3% hydrogen peroxide solution. For exposure experiments, we used a previously collected, processed, and characterized 101 sediment extract (Elizabeth River sediment extract, ERSE) from the Atlantic Woods Industries Superfund site, a former creosote wood treatment facility, in the Elizabeth River (VA, USA). This extract is a real-world mixture of water and suspended solids with a total PAH content of 5,073 ng/mL PAH, summed from analyses of 36 different PAH. We exposed half of the embryos in each group to 5% ERSE (diluted in 20% ASW) and the remaining half to clean water only. We chose this ERSE concentration based on previous studies showing CYP induction in both sensitive and tolerant mummichog with no lethality in sensitive fish. We dosed embryos in 20 mL glass scintillation vials (VWR, Westchester, PA, USA) at 27 °C beginning at 24 h post-fertilization (hpf). After 14 days, we flash froze embryos in liquid nitrogen and stored at -80 °C. We dissected liver tissue from depurated, wild-caught adult fish, flash froze tissue in liquid nitrogen and stored at -80 °C. Embryos from each population were randomly assigned to treatment or control groups by a blinded researcher. All care, reproductive techniques and rearing techniques were non-invasive. All vertebrate animal experiments were performed in accordance with all relevant guidelines and regulations following a protocol approved by the Duke University Institutional Animal Care and Use Committee (A139-16-06).

#### **Genomic DNA isolation**

We extracted genomic DNA from adult liver tissue with DNeasy Blood & Tissue Kits (cat. No. 69504, Qiagen, Hilden, Germany). Briefly, we cut  $\sim\!20$  mg of liver tissue over dry ice. We added 180  $\mu L$  of buffer ATL, minced the tissue over wet ice and transferred the sample to a 1.5mL safe lock tube. After adding 20  $\mu L$  of Proteinase K, we incubated samples at 56 °C overnight. We followed the kit protocol for on-column purification, and eluted the final genomic DNA in 200  $\mu L$  milliq-H $_2$ O and incubated at room temperature before centrifuging at 8,000 rpm for 1 min and storing at -20 °C.

#### CYP1A resequencing and contig assembly

We re-sequenced the CYP1A gene and 7Kb upstream of the CYP1A TSS via primer walking and Sanger sequencing in N=4 wild-caught adult mummichog, one male and one female each randomly selected from samples derived from PAH-tolerant and -sensitive populations. The completed sequence spans chromosomal coordinates chr4:1,265,806-1,276,399 (NCBI RefSeq assembly Fundulus\_heteroclitus-3.0.2 (2015), accession NW\_012234324.1). We performed PCR in 12.5-25 µl reactions using Platinum SuperFi II Green PCR Master Mix (#12359010; Thermo Fisher Scientific, Waltham, MD), 0.5 µl of sample DNA, and forward and reverse primers to a final concentration of 500nM on a Biometra T Advanced Thermocycler (Analytik Jena, Jena, Germany) under the following conditions: 98 °C for 30 s, followed by 35 cycles of 98 °C for 5 s, primer annealing temperature for 20 s, extension at 72 °C for 30 s, with a final extension at 72 °C for 5 min. We diluted the products 1:4 with MilliQ-H<sub>2</sub>O and submitted them for Sanger sequencing through the OHSU Vollum DNA Sequencing Core using an ABI (Applied Biosystems) 3730xl 96-capillary DNA Analyzer. We manually edited the resulting ABI files before assembling overlapping sequences into contigs utilizing the PRABI Cap3 Sequence Assembly Program (https://doua.prabi.fr/software/cap3) and aligned contigs and the published reference sequence (GCF\_000826765.1) using the CLUSTALW Multiple Sequence Alignment tool (https://www.genom e.jp/tools-bin/clustalw). We analyzed the resulting alignments via the FIMO tool within the MEME Suite to identify transcription factor motifs (https://meme-suite.org/meme/tools/fimo) using published TFBS consensus sequences for AHR<sup>102</sup>, GR<sup>103</sup>, Sp1<sup>104,105</sup>, HNF-3<sup>106</sup>, CREB<sup>107</sup>, and NF-I<sup>108,109</sup>.

#### Total RNA isolation and cDNA synthesis

We extracted total RNA from both adult and embryo mummichog samples using the following protocol. Briefly, we cut ~ 10 mg of liver tissue or minced whole embryo pools over dry ice. We placed samples into round bottom 2mL safe lock tubes with 1mL of TRI Reagent (cat. no. T9424; Sigma-Aldrich, St. Louis, MO, USA) containing 1% (v/v) molecular biology grade β-mercaptoethanol (cat. no. M3148; Sigma-Aldrich, St. Louis, MO, USA). We homogenized samples with 5 mm stainless steel beads via two 2-minute 25 Hz bursts in a TissueLyser system (cat. no. 85210; Qiagen, Hilden, Germany). We transferred lysates to 1.5mL tubes, incubated samples at room temperature for 5 min, added 200 µl of Chloroform (cat. no. 25666; Sigma-Aldrich, St. Louis, MO, USA), mixed thoroughly, transferred tissue digests into 2mL 5PRIME Phase Lock Gel Heavy tubes (cat. no. 2302830; Quantabio, Beverly, MA, USA), incubated at room temperature for 3 min, and centrifuged at 10,000 rpm for 15 min at 4 °C. We transferred supernatants to new 1.5 mL tubes and precipitated RNA using 10% (v/v) 3 M sodium acetate (pH 5.5) (cat. no. AM9740; Invitrogen, Waltham, MA, USA), molecular biology grade glycogen to a final concentration of 1 µg/µl (cat. no. R0561; Thermo Scientific, Waltham, MA, USA), and 100% ethanol for at least 10 min at -20 °C. We pelleted RNA at 11,000 rpm for 10 min at 4 °C, washed the pellet twice with 75% ethanol, and resuspended in MilliQ water. We synthesized cDNA with qScript cDNA SuperMix kits (cat. no. 95048; Quantabio, Beverly, MA, USA) on Biometra TAdvanced Thermocyclers (cat. no. 846-x-070-280; Analytik Jena, Jena, Germany), quantified cDNA using Quant-iT RNA Assay (cat. no. Q10213; Invitrogen, Waltham, MA) and Quant-iT PicoGreen dsDNA Assay Kits (cat. no. P7589; Invitrogen, Waltham, MA) to quantify both cDNA concentration and possible interfering cDNA-RNA hybrids, respectively. We used these measurements to standardize samples to a concentration of 50 ng/µl for input into real-time qPCR. All samples were randomized to experimental batch using a random number generator.

#### Real-time qPCR for gene expression

We measured gene expression of *CYP1A*, *CYP1B* and *CYP1C* genes using the following protocol. Briefly, we performed qPCR on cDNA generated from total RNA isolated from adult liver tissue (*N*=5 males and *N*=5 females per population) and embryos (*N*=3 pools of 10 embryos per population per exposure status). We designed primers spanning exon-exon junctions that captured all known gene isoforms using the NCBI Primer-BLAST tool (CYP1A forward 5′- GACCTCTTTGGAGCTGGTTT – 3′, reverse 5′- CCAGACCGACTTTCTC CTTGATT – 3′, 124 bp product; CYP1B forward 5′- ATATTTGGAGCCAGCCAGGAC – 3′, reverse 5′- GTAC TTGACAAAAATGAGGATGATCCACTG – 3′, 69 bp product; CYP1C forward 5′- AGCCAGGGCATGACAT CAAC – 3′, reverse 5′- ACACGATGACCAGGAGTTCAG – 3′, 96 bp product). We ran qPCR in 10 µl reactions in triplicate with PerfeCTa SYBR Green FastMix (cat. no. 95072-012; Quantabio, Beverly, MA), 50 ng cDNA, and 500 nM forward and reverse primers on a qTower³G real-time thermal cycler (Analytik Jena, Jena, Germany)

under the following conditions: 95 °C for 30 s, followed by 44 cycles of 95 °C for 5 s, annealing temperature for 30 s (CYP1A=65 °C, CYP1B=60 °C, CYP1C=50 °C), with a final melt curve analysis to confirm single products. We calculated cycles to threshold (C(t)) with qPCRsoftv.4.0 and averaged sample triplicate values (standard deviation  $\leq$ 0.5). We were unable to validate a reference ("housekeeping") gene as invariant across populations and exposure status; therefore, we report relative fold-change values (PAH-tolerant relative to PAH-sensitive). All samples were randomized to experimental batch using a random number generator.

#### Chromatin immunoprecipitation (ChIP) assays

We characterized histone modifications at the CYP1A proximal promoter-enhancer via ChIP-qPCR. Prior to ChIP experiments, we confirmed antibody specificity and efficiency with EpiCypher designer recombinant nucleosome panels (SNAP-ChIP K-MetStat Panel, cat. no. 19-1001) (Supp. Table 27). We performed ChIP-qPCR on four regions of CYP1A: three AHR-binding xenobiotic response elements (XREs) in the proximal promoterenhancer, plus the transcription start site (TSS) for three histone modifications (H3K4me1, H3K4me3, and H3K27me3) on N=5 pools of 10 embryos each per population per exposure and on N=5 adult male liver samples per population using the following antibodies (H3K4me1, cat. no. 13-0040, Epicypher, Durham, NC; H3K4me3, cat. no. 13-0041, Epicypher, Durham, NC; H3K27me3, cat. no. MA5-1198, Invitrogen, Carlsbad, CA). We adapted the MAGnify Chromatin Immunoprecipitation System (cat. no. 49-2024, Invitrogen, Carlsbad, CA, USA) protocol for ChIP-qPCR. Briefly, we minced either 50 mg of adult liver tissue or whole embryo pools with razor blades over ice with 250 µL of chilled 1X PBS, crosslinked chromatin with 37% formaldehyde (cat. no. BP531-25, Fisher Scientific, Hampton, NJ, USA) diluted with PBS to a final concentration of 1%, incubated samples for 5 min, quenched reactions with 1.25 M glycine to a final concentration of 0.125 M, and homogenized samples with 0.5 mm stainless steel beads via two 2-minute, 25 Hz bursts on a TissueLyser (cat. no. 85210; Qiagen, Hilden, Germany) before immediately transferring to a DNA LoBind Tube 1.5 ml (cat. no. 022431021, Eppendorf, Hamburg, Germany). We pelleted samples at 1,4000 rpm for 10 min at 4 °C, washed pellets with 500 µl chilled PBS, and centrifuged at 4,000 rpm for 10 min 4 °C. We lysed cells with lysis buffer supplemented with protease inhibitors and mechanically sheared chromatin to 200-500 bp fragments (median fragment sizes 394-536 bp in all samples) in Covaris fiber pre-slit microtubes (cat. no. 520045, Covaris, Woburn, MA, USA) with a Covaris S220 sonicator (50 μl sample, temperature 3-9 °C, peak incidence power 105 W, 200 cycles per burst, duty factor 1%, for a total of 450 s). We verified fragment lengths on a QIAxcel Advanced system (Qiagen, Hilden, Germany) using the QIAXcel High Resolution kit (cat. no. 929002), Qiagen 15 bp-3 kb alignment marker (cat. no. 929522), and Qiagen 100 - 2.5 kB size marker (cat. no. 929559) using smear detection M400 method settings and stored sonicated chromatin at -80 °C. We performed antibody enrichment with 1 µg antibody per ChIP reaction, IgG negative controls, and Epicypher SNAP-ChIP nucleosomes as spike-in positive controls. We bound chromatin to the magnetic dynabeads, washed the bound chromatin, reversed the chromatin crosslinks, purified the chromatin, and eluted 195 µl of DNA Elution Buffer and stored samples at -20 °C. We quantified enrichment of each histone PTM at each CYP1A region using qPCR in triplicate (10 µl DNA input, annealing temperature 50 °C for all reactions, with the following primer sets: XRE3 forward 5'- CGGTTTGATCACTG CGCTCT – 3', reverse 5' - TCTCCGCGGGAGTTAAAGAT – 3', 54 bp product; XRE2 forward 5' - AACTCC CGCGGAGAGCATGC -3', reverse 5'- AAGGTTGCGCAGTGCTGATA -3', 69 bp product; XRE1 forward 5'- AAGGCGGTAGACACTTTGT - 3', reverse 5'- GCCATGAATGAAGTTTGGAGCA - 3', 110 bp product; TSS forward 5'- GTAGCCAATAAGATTGCGCAGC -3', reverse 5'- AATTCCAGAGATGCGTGTCCAA -3', 130 bp product). We evaluated ChIP performance by pooling samples from each ChIP experimental batch and running qPCR for Epicypher nucleosome barcodes specific to on-target modified nucleosomes (H3K4me1, H3K4me3, and H3K27me3) and unmodified nucleosomes (H3K4me0 and H3K27me0, respectively). All samples were randomized to experimental batch using a random number generator.

#### Statistical analysis

To analyze gene expression data, we stratified raw C(t) data by embryo or adult status, by sex (for adults only), by treatment (for embryos only), and by target gene (CYP1A, CYP1B, CYP1C). In embryo data, we evaluated difference-in-difference (D-i-D) in each gene's expression response to PAH challenge between PAH-tolerant and PAH-sensitive populations, denoted as [PAH-tolerant (treatment-control)] - [PAH-sensitive (treatmentcontrol)]. In adult data, we evaluated D-i-D in sex differences in each gene's expression between PAH-tolerant and PAH-sensitive populations, denoted as [PAH-tolerant (males - females)] - [PAH-sensitive (males - females)]. We chose Hedge's g as a sample-sized corrected Cohen's d value (recommended for samples N < 20)<sup>57</sup>. Here, Hedge's g values refer to differences in least squared means in terms of standard deviations. We computed D-i-D values following Feingold's<sup>110</sup> approach; we first computed Hedge's g for each Difference (e.g., treatment-control for each population), based on raw standard deviations, and then subtracted Hedge's g values for each population group to yield final D-i-D estimates. We applied a series of independent sample t-tests and computed Hedge's g for treatment and sex effects within each population group (PAH-tolerant and PAH-sensitive), respectively. Next, we subtracted the Hedge's g values between each population group, as outlined above, to yield D-i-D Hedge's g estimates. Hedge's g estimates of effect size can be interpreted as follows: 0.2 - small effect, 0.4-0.6 - moderate effect, > 0.8 - large effect. We calculated 95% confidence intervals around the D-i-D effect sizes (if the confidence interval does not contain zero, then the effect sizes can be interpreted as statistically significant at p < 0.05). We tested for differences in basal CYP1A expression between PAH-tolerant and PAH-sensitive embryos with an independent samples t-test. These analyses were conducted in SPSS Version 29.0 (IBM Corp., Armonk, NY), R Studio (using the "psych" R package) and Microsoft Excel.

To analyze ChIP data, we stratified fold-change values (relative to IgG negative controls) by embryo or adult status, by treatment (for embryos only), and by target region (XRE3, XRE2, XRE1, TA/TSS). Each sample ID contained four repeated measures, one for each region within the *CYP1A* proximal promoter-enhancer, and each

ChIP assay was run in one of several experimental batches. Therefore, there were two dependencies in the data that may have biased results run with traditional tests (e.g., independent samples t-tests). Therefore, we ran a series of three mixed models each for embryo and adult datasets, respectively, including main effects for population group and for treatment (embryo only), an interaction term between population group and treatment (embryo only), covariates for experimental batch and gene region, and a random intercept to account for correlation among gene regions within a sample ID, nested within experimental batch. In addition, we included a three-way interaction term (population group\*treatment\*gene region) for embryo data and a two-way interaction term (population group\*gene region) for adult data, to estimate least squares means for fold-change values for each region for a given treatment group in each population group. Given the small sample and high variability in the data, instead of directly interpreting model results, we computed statistical effect sizes (Hedge's g) for each hypothesized difference (e.g., [PAH-tolerant - PAH-sensitive] for each gene region within adult data) and for each hypothesized D-i-D (e.g., [PAH-tolerant (treatment-control)] - [PAH-sensitive (treatment-control)] for each gene region within embryo data). We computed 95% confidence intervals for each Difference and D-i-D estimate. In addition, we computed differences in fold-change ratios (H3K27me3/H3K4me3 and H3K27me3/ H3K4me1) by computing ratios from fold-change values and replicating the prior analyses. Although batches were assay-specific, in some cases, there was complete or near-complete overlap in batches when computing ratios. In these instances, we chose one assay within each batch as an indicator to control for experimental batch. We conducted a sensitivity analysis for this approach by running tests for the H3K27me3/H3K4me1 ratio twice, using either assay as the batch indicator, and observed no difference in results. These analyses were conducted in SAS Version 9.4 (Cary, NC), R Studio (using the "psych" R package) and Microsoft Excel.

#### ARRIVE guidelines compliance

All experiments and statistical analyses reported in this manuscript were performed in compliance with the ARRIVE guidelines (https://arriveguidelines.org).

#### Data availability

All data generated or analyzed during this study are included in this published article (and its Supplementary Information files).

Received: 28 August 2024; Accepted: 9 December 2024

#### Published online: 24 January 2025

#### References

- 1. Toxicological profile for polycyclic aromatic hydrocarbons. Agency for Toxic Substances and Disease Registry, U.S. Department of Health and Human Services, Public Health Service (Atlanta, 1995).
- 2. Diesel and Gasoline Engine Exhausts and Some Nitroarenes. IARC monographs on the evaluation of carcinogenic risks to humans. IARC Monogr. Eval Carcinog. Risks Hum. 105, 9–699 (2014).
- 3. IARC Monographs on the Identification of Carcinogenic Hazards to Humans. Report of the Advisory Group to Recommend Priorities for the IARC Monographs During 2020–2024 (2019).
- 4. Outdoor Air Pollution. IARC working group on the evaluation of carcinogenic risks to humans. *IARC Monogr. Eval Carcinog. Risks Hum.* **109**, 9–444 (2016).
- Tobacco Smoke and Involuntary Smoking. IARC working group on the evaluation of carcinogenic risks to humans. IARC Monogr. Eval Carcinog. Risks Hum. 83, 1–1438 (2004).
- DeMarini, D. M. & Linak, W. P. Mutagenicity and carcinogenicity of combustion emissions are impacted more by combustor technology than by fuel composition: A brief review. *Environ. Mol. Mutagen.* 63, 135–150. https://doi.org/10.1002/em.22475 (2022).
- Programme, U. N. E. Spreading like Wildfire: The rising threat of extraordinary Landscape fires. UNEP Rapid Response Assess. Nairobi (2022).
- 8. Albert, R. E. Comparative carcinogenic potencies of particulates from diesel engine exhausts, coke oven emissions, roofing tar aerosols and cigarette smoke. *Environ. Health Perspect.* 47, 339–341. https://doi.org/10.1289/ehp.8347339 (1983).
- Cupitt, L. T., Glen, W. G. & Lewtas, J. Exposure and risk from ambient particle-bound pollution in an airshed dominated by residential wood combustion and mobile sources. *Environ. Health Perspect.* 102 (Suppl 4), 75–84. https://doi.org/10.1289/ehp.94 102s475 (1994).
- 10. Baan, R. A., Stewart, B. W. & Straif, K. (eds) in Tumour Site Concordance and Mechanisms of Carcinogenesis IARC Scientific Publications (2019).
- The, L. Lung cancer: some progress, but still a lot more to do. Lancet 394, 1880. https://doi.org/10.1016/S0140-6736(19)32795-3 (2019).
- 12. Frick, C. et al. Quantitative estimates of preventable and treatable deaths from 36 cancers worldwide: A population-based study. Lancet Glob Health. 11, e1700–e1712. https://doi.org/10.1016/S2214-109X(23)00406-0 (2023).
- 13. Sung, H. et al. Global Cancer statistics 2020: GLOBOCAN estimates of incidence and mortality worldwide for 36 cancers in 185 countries. *CA Cancer J. Clin.* 71, 209–249. https://doi.org/10.3322/caac.21660 (2021).
- 14. Ferlay, J. et al. Cancer statistics for the year 2020: an overview. *Int. J. Cancer*. https://doi.org/10.1002/ijc.33588 (2021).
- 15. Ferlay, J. et al. Global cancer observatory: Cancer today. in International Agency for Research on Cancer, Lyon, France (2024).
- Stading, R., Gastelum, G., Chu, C., Jiang, W. & Moorthy, B. Molecular mechanisms of pulmonary carcinogenesis by polycyclic aromatic hydrocarbons (PAHs): Implications for human lung cancer. Semin Cancer Biol. 76, 3–16. https://doi.org/10.1016/j.sem cancer.2021.07.001 (2021).
- 17. Gastelum, G. et al. Polycyclic aromatic hydrocarbon-induced pulmonary carcinogenesis in cytochrome P450 (CYP)1A1- and 1A2-Null mice: roles of CYP1A1 and CYP1A2. *Toxicol. Sci.* 177, 347–361. https://doi.org/10.1093/toxsci/kfaa107 (2020).
- 18. Shimada, T., Oda, Y., Gillam, E. M., Guengerich, F. P. & Inoue, K. Metabolic activation of polycyclic aromatic hydrocarbons and other procarcinogens by cytochromes P450 1A1 and P450 1B1 allelic variants and other human cytochromes P450 in Salmonella typhimurium NM2009. *Drug Metab. Dispos.* 29, 1176–1182 (2001).
- 19. Shimada, T. & Fujii-Kuriyama, Y. Metabolic activation of polycyclic aromatic hydrocarbons to carcinogens by cytochromes P450 1A1 and 1B1. *Cancer Sci.* **95**, 1–6. https://doi.org/10.1111/j.1349-7006.2004.tb03162.x (2004).

- 20. Shimada, T. et al. Arylhydrocarbon receptor-dependent induction of liver and lung cytochromes P450 1A1, 1A2, and 1B1 by polycyclic aromatic hydrocarbons and polychlorinated biphenyls in genetically engineered C57BL/6J mice. *Carcinogenesis* 23, 1199–1207. https://doi.org/10.1093/carcin/23.7.1199 (2002).
- 21. Matsumoto, Y. et al. Aryl hydrocarbon receptor plays a significant role in mediating airborne particulate-induced carcinogenesis in mice. *Environ. Sci. Technol.* 41, 3775–3780. https://doi.org/10.1021/es062793g (2007).
- 22. Willett, K. L., Gardinali, P. R., Sericano, J. L., Wade, T. L. & Safe, S. H. Characterization of the H4IIE rat hepatoma cell bioassay for evaluation of environmental samples containing polynuclear aromatic hydrocarbons (PAHs). *Arch. Environ. Contam. Toxicol.* 32, 442–448. https://doi.org/10.1007/s002449900211 (1997).
- 23. Till, M., Riebniger, D., Schmitz, H. J. & Schrenk, D. Potency of various polycyclic aromatic hydrocarbons as inducers of CYP1A1 in rat hepatocyte cultures. *Chem. Biol. Interact.* 117, 135–150. https://doi.org/10.1016/s0009-2797(98)00105-7 (1999).
- Machala, M., Vondracek, J., Blaha, L., Ciganek, M. & Neca, J. V. Aryl hydrocarbon receptor-mediated activity of mutagenic polycyclic aromatic hydrocarbons determined using in vitro reporter gene assay. *Mutat. Res.* 497, 49–62. https://doi.org/10.1016/s1383-5718(01)00240-6 (2001).
- 25. Malhotra, J., Malvezzi, M., Negri, E., La Vecchia, C. & Boffetta, P. Risk factors for lung cancer worldwide. Eur. Respir J. 48, 889–902. https://doi.org/10.1183/13993003.00359-2016 (2016).
- Bach, P. B. et al. Variations in lung cancer risk among smokers. J. Natl. Cancer Inst. 95, 470–478. https://doi.org/10.1093/jnci/95. 6.470 (2003).
- 27. Gabriel, A. A. G. et al. Genetic analysis of Lung Cancer and the germline impact on somatic mutation burden. *J. Natl. Cancer Inst.* 114, 1159–1166. https://doi.org/10.1093/jnci/djac087 (2022).
- 28. Sengupta, D. et al. A comprehensive meta-analysis and a case-control study give insights into genetic susceptibility of lung cancer and subgroups. Sci. Rep. 11, 14572. https://doi.org/10.1038/s41598-021-92275-z (2021).
- 29. Ezzeldin, N. et al. Genetic polymorphisms of human cytochrome P450 CYP1A1 in an Egyptian population and tobacco-induced lung cancer. *Genes Environ.* 39, 7. https://doi.org/10.1186/s41021-016-0066-4 (2017).
- 30. Zhang, L. P., Wang, C. P., Li, L. H., Tang, Y. F. & Li, W. C. The interaction between smoking and CYP1A1 MspI polymorphism on lung cancer: A meta-analysis in the Chinese population. Eur. J. Cancer Care (Engl). 26. https://doi.org/10.1111/ecc.12459 (2017).
- 31. He, X. F. et al. Association between the CYP1A1 T3801C polymorphism and risk of cancer: Evidence from 268 case-control studies. *Gene* 534, 324–344 (2014).
- 32. Nakachi, K., Imai, K., Hayashi, S., Watanabe, J. & Kawajiri, K. Genetic susceptibility to squamous cell carcinoma of the lung in relation to cigarette smoking dose. *Cancer Res.* 51, 5177–5180 (1991).
- 33. Kawajiri, K., Nakachi, K., Imai, K., Hayashi, S. & Watanabe, J. Individual differences in lung cancer susceptibility in relation to polymorphisms of P-450IA1 gene and cigarette dose. *Princess Takamatsu Symp.* 21, 55–61 (1990).
- 34. Nebert, D. W., McKinnon, R. A. & Puga, A. Human drug-metabolizing enzyme polymorphisms: Effects on risk of toxicity and cancer. DNA Cell. Biol. 15, 273–280. https://doi.org/10.1089/dna.1996.15.273 (1996).
- 35. Shah, P. P., Saurabh, K., Pant, M. C., Mathur, N. & Parmar, D. Evidence for increased cytochrome P450 1A1 expression in blood lymphocytes of lung cancer patients. *Mutat. Res.* 670, 74–78. https://doi.org/10.1016/j.mrfmmm.2009.07.006 (2009).
- Schwarz, D., Kisselev, P., Cascorbi, I., Schunck, W. H. & Roots, I. Differential metabolism of benzo[a]pyrene and benzo[a]pyrene-7,8-dihydrodiol by human CYP1A1 variants. Carcinogenesis 22, 453–459. https://doi.org/10.1093/carcin/22.3.453 (2001).
- 37. Hayashi, S., Watanabe, J., Nakachi, K. & Kawajiri, K. Genetic linkage of lung cancer-associated MspI polymorphisms with amino acid replacement in the heme binding region of the human cytochrome P450IA1 gene. *J. Biochem.* 110, 407–411. https://doi.org/10.1093/oxfordjournals.jbchem.a123594 (1991).
- 38. Cosma, G., Crofts, F., Taioli, E., Toniolo, P. & Garte, S. Relationship between genotype and function of the human CYP1A1 gene. J. Toxicol. Environ. Health. 40, 309–316. https://doi.org/10.1080/15287399309531796 (1993).
- Ishibe, N. et al. Susceptibility to lung cancer in light smokers associated with CYP1A1 polymorphisms in mexican- and africanamericans. Cancer Epidemiol. Biomarkers Prev. 6, 1075–1080 (1997).
- 40. Van Veld, P. A. J. evidence for depression of cytochrome P4501A in a population of chemically resistant mummichog (Fundulus heteroclitus). *Environ. Sci.* **3**, 221–234 (1995).
- 41. Meyer, J. N., Nacci, D. E. & Di Giulio, R. T. Cytochrome P4501A (CYP1A) in killifish (Fundulus heteroclitus): Heritability of altered expression and relationship to survival in contaminated sediments. *Toxicol. Sci.* 68, 69–81. https://doi.org/10.1093/toxsci/68.1.69 (2002).
- 42. Meyer, J. N., Wassenberg, D. M., Karchner, S. I., Hahn, M. E. & Di Giulio, R. T. Expression and inducibility of aryl hydrocarbon receptor pathway genes in wild-caught killifish (Fundulus heteroclitus) with different contaminant-exposure histories. *Environ. Toxicol. Chem.* 22, 2337–2343. https://doi.org/10.1897/02-495 (2003).
- 43. Wills, L. P., Matson, C. W., Landon, C. D. & Di Giulio, R. T. Characterization of the recalcitrant CYP1 phenotype found in Atlantic killifish (Fundulus heteroclitus) inhabiting a Superfund site on the Elizabeth River, VA. *Aquat. Toxicol.* **99**, 33–41. https://doi.org/10.1016/j.aquatox.2010.03.015 (2010).
- 44. Clark, B. W., Bone, A. J. & Di Giulio, R. T. Resistance to teratogenesis by F1 and F2 embryos of PAH-adapted Fundulus heteroclitus is strongly inherited despite reduced recalcitrance of the AHR pathway. *Environ. Sci. Pollut Res. Int.* 21, 13898–13908. https://doi.org/10.1007/s11356-013-2446-7 (2014).
- 45. Di Giulio, R. T. & Clark, B. W. The Elizabeth river story: A case study in evolutionary toxicology. *J. Toxicol. Environ. Health B Crit. Rev.* 18, 259–298. https://doi.org/10.1080/15320383.2015.1074841 (2015).
- Reid, N. M. et al. The genomic landscape of rapid repeated evolutionary adaptation to toxic pollution in wild fish. Science 354, 1305–1308. https://doi.org/10.1126/science.aah4993 (2016).
- 47. Wills, L. P. et al. Comparative chronic liver toxicity of benzo[a]pyrene in two populations of the atlantic killifish (Fundulus heteroclitus) with different exposure histories. *Environ. Health Perspect.* 118, 1376–1381. https://doi.org/10.1289/ehp.0901799 (2010).
- 48. Meyer, J. N. & Di Giulio, R. T. Heritable adaptation and fitness costs in killifish (Fundulus heteroclitus) inhabiting a polluted estuary. *Ecol. Appl.* 13, 490–503 (2003).
- 49. Ptashne, M. Binding reactions: epigenetic switches, signal transduction and cancer. Curr. Biol. 19, R234–241. https://doi.org/10.1016/j.cub.2009.02.015 (2009).
- 50. Ptashne, M. On the use of the word 'epigenetic'. Curr. Biol. 17, R233-236. https://doi.org/10.1016/j.cub.2007.02.030 (2007).
- 51. Henikoff, S. & Greally, J. M. Epigenetics, cellular memory and gene regulation. Curr. Biol. 26, R644–648. https://doi.org/10.1016/j.cub.2016.06.011 (2016).
- Bernstein, B. E., Meissner, A. & Lander, E. S. The mammalian epigenome. Cell 128, 669–681. https://doi.org/10.1016/j.cell.2007. 01.033 (2007).
- 53. Haghani, A. et al. DNA methylation networks underlying mammalian traits. *Science* **381**, eabq5693. https://doi.org/10.1126/science.abq5693 (2023).
- 54. Takahashi, Y. et al. Transgenerational inheritance of acquired epigenetic signatures at CpG islands in mice. Cell 186, 715–731 e719. https://doi.org/10.1016/j.cell.2022.12.047 (2023).
- 55. Reveron-Gomez, N. et al. Accurate recycling of parental histones reproduces the histone modification landscape during DNA replication. *Mol Cell* 72, 239–249 e235. https://doi.org/10.1016/j.molcel.2018.08.010 (2018).
- Flury, V. et al. Recycling of modified H2A-H2B provides short-term memory of chromatin states. Cell 186, 1050–1065 e1019. https://doi.org/10.1016/j.cell.2023.01.007 (2023).

- 57. Lakens, D. Calculating and reporting effect sizes to facilitate cumulative science: A practical primer for t-tests and ANOVAs. *Front. Psychol.* 4, 863. https://doi.org/10.3389/fpsyg.2013.00863 (2013).
- 58. Jirtle, R. L. & Skinner, M. K. Environmental epigenomics and disease susceptibility. *Nat. Rev. Genet.* **8**, 253–262. https://doi.org/10.1038/nrg2045 (2007).
- 59. Timme-Laragy, A. R., Meyer, J. N., Waterland, R. A. & Di Giulio, R. T. Analysis of CpG methylation in the killifish CYP1A promoter. *Comp. Biochem. Physiol. C Toxicol. Pharmacol.* 141, 406–411. https://doi.org/10.1016/j.cbpc.2005.09.009 (2005).
- Wang, H. et al. H3K4me3 regulates RNA polymerase II promoter-proximal pause-release. Nature 615, 339–348. https://doi.org/ 10.1038/s41586-023-05780-8 (2023).
- 61. Kubo, N. et al. H3K4me1 facilitates promoter-enhancer interactions and gene activation during embryonic stem cell differentiation. *Mol. Cell.* https://doi.org/10.1016/j.molcel.2024.02.030 (2024).
- 62. Coleman, R. T. & Struhl, G. Causal role for inheritance of H3K27me3 in maintaining the OFF state of a Drosophila HOX gene. *Science* 356. https://doi.org/10.1126/science.aai8236 (2017).
- 63. Sankar, A. et al. Histone editing elucidates the functional roles of H3K27 methylation and acetylation in mammals. *Nat. Genet.* 54, 754–760. https://doi.org/10.1038/s41588-022-01091-2 (2022).
- Scacchetti, A. & Bonasio, R. Histone gene editing probes functions of H3K27 modifications in mammals. Nat. Genet. 54, 746

  747. https://doi.org/10.1038/s41588-022-01096-x (2022).
- Bernstein, B. E. et al. A bivalent chromatin structure marks key developmental genes in embryonic stem cells. Cell 125, 315–326. https://doi.org/10.1016/j.cell.2006.02.041 (2006).
- Voigt, P., Tee, W. W. & Reinberg, D. A double take on bivalent promoters. Genes Dev. 27, 1318–1338. https://doi.org/10.1101/gad .219626.113 (2013).
- Nalabothula, N. et al. Archaeal nucleosome positioning in vivo and in vitro is directed by primary sequence motifs. BMC Genom. 14, 391. https://doi.org/10.1186/1471-2164-14-391 (2013).
- Meyer, J. N., Volz, D. C., Freedman, J. H. & Di Giulio, R. T. Differential display of hepatic mRNA from killifish (Fundulus heteroclitus) inhabiting a Superfund estuary. *Aquat. Toxicol.* 73, 327–341. https://doi.org/10.1016/j.aquatox.2005.03.022 (2005).
- Burrill, D. R., Inniss, M. C., Boyle, P. M. & Silver, P. A. Synthetic memory circuits for tracking human cell fate. *Genes Dev.* 26, 1486–1497. https://doi.org/10.1101/gad.189035.112 (2012).
- 70. Azuara, V. et al. Chromatin signatures of pluripotent cell lines. Nat. Cell. Biol. 8, 532-538. https://doi.org/10.1038/ncb1403 (2006).
- Shema, E. et al. Single-molecule decoding of combinatorially modified nucleosomes. Science 352, 717–721. https://doi.org/10.11 26/science.aad7701 (2016).
- Blanco, E., Gonzalez-Ramirez, M., Alcaine-Colet, A., Aranda, S. & Di Croce, L. The bivalent genome: Characterization, structure, and Regulation. *Trends Genet.* 36, 118–131 (2020).
- Bracken, A. P., Dietrich, N., Pasini, D., Hansen, K. H. & Helin, K. Genome-wide mapping of polycomb target genes unravels their roles in cell fate transitions. Genes Dev. 20, 1123–1136. https://doi.org/10.1101/gad.381706 (2006).
- 74. Caretti, G., Di Padova, M., Micales, B., Lyons, G. E. & Sartorelli, V. The polycomb Ezh2 methyltransferase regulates muscle gene expression and skeletal muscle differentiation. *Genes Dev.* 18, 2627–2638. https://doi.org/10.1101/gad.1241904 (2004).
- Cui, K. et al. Chromatin signatures in multipotent human hematopoietic stem cells indicate the fate of bivalent genes during differentiation. Cell. Stem Cell. 4, 80–93. https://doi.org/10.1016/j.stem.2008.11.011 (2009).
- Ezhkova, E. et al. Ezh2 orchestrates gene expression for the stepwise differentiation of tissue-specific stem cells. Cell 136, 1122–1135. https://doi.org/10.1016/j.cell.2008.12.043 (2009).
- 77. Rahl, P. B. et al. c-Myc regulates transcriptional pause release. Cell 141, 432-445. https://doi.org/10.1016/j.cell.2010.03.030 (2010).
- 78. Su, I. H. et al. Ezh2 controls B cell development through histone H3 methylation and igh rearrangement. *Nat. Immunol.* 4, 124–131. https://doi.org/10.1038/ni876 (2003).
- Lee, M. G. et al. Demethylation of H3K27 regulates polycomb recruitment and H2A ubiquitination. Science 318, 447–450. https://doi.org/10.1126/science.1149042 (2007).
- Agger, K. et al. UTX and JMJD3 are histone H3K27 demethylases involved in HOX gene regulation and development. *Nature* 449, 731–734. https://doi.org/10.1038/nature06145 (2007).
- 81. Mikkelsen, T. S. et al. Genome-wide maps of chromatin state in pluripotent and lineage-committed cells. *Nature* **448**, 553–560. https://doi.org/10.1038/nature06008 (2007).
- 82. Mohn, F. et al. Lineage-specific polycomb targets and de novo DNA methylation define restriction and potential of neuronal progenitors. *Mol. Cell.* 30, 755–766. https://doi.org/10.1016/j.molcel.2008.05.007 (2008).
- 83. Harikumar, A. & Meshorer, E. Chromatin remodeling and bivalent histone modifications in embryonic stem cells. *EMBO Rep.* 16, 1609–1619. https://doi.org/10.15252/embr.201541011 (2015).
- 84. Tian, Y. et al. Early Life Short-Term exposure to Polychlorinated Biphenyl 126 in mice leads to metabolic dysfunction and microbiota changes in Adulthood. *Int. J. Mol. Sci.* 23. https://doi.org/10.3390/ijms23158220 (2022).
- 85. Jiang, W. et al. Persistent induction of cytochrome P450 (CYP)1A enzymes by 3-methylcholanthrene in vivo in mice is mediated by sustained transcriptional activation of the corresponding promoters. *Biochem. Biophys. Res. Commun.* **390**, 1419–1424. https://doi.org/10.1016/j.bbrc.2009.11.021 (2009).
- 86. Fazili, I. S. et al. Persistent induction of cytochrome P4501A1 in human hepatoma cells by 3-methylcholanthrene: Evidence for sustained transcriptional activation of the CYP1A1 promoter. *J. Pharmacol. Exp. Ther.* 333, 99–109. https://doi.org/10.1124/jpet. 109.162222 (2010).
- 87. Amenya, H. Z., Tohyama, C. & Ohsako, S. Dioxin induces Ahr-dependent robust DNA demethylation of the Cyp1a1 promoter via Tdg in the mouse liver. Sci. Rep. 6, 34989. https://doi.org/10.1038/srep34989 (2016).
- 88. Ciolino, H. P. & Yeh, G. C. Inhibition of aryl hydrocarbon-induced cytochrome P-450 1A1 enzyme activity and CYP1A1 expression by resveratrol. *Mol. Pharmacol.* **56**, 760–767 (1999).
- 89. Ciolino, H. P. & Yeh, G. C. The flavonoid galangin is an inhibitor of CYP1A1 activity and an agonist/antagonist of the aryl hydrocarbon receptor. *Br. J. Cancer.* **79**, 1340–1346. https://doi.org/10.1038/sj.bjc.6690216 (1999).
- Ciolino, H. P., Daschner, P. J. & Yeh, G. C. Dietary flavonols quercetin and kaempferol are ligands of the aryl hydrocarbon receptor that affect CYP1A1 transcription differentially. Biochem. J. 340 (Pt 3), 715–722 (1999).
- 91. Ciolino, H. P., Wang, T. T. & Yeh, G. C. Diosmin and diosmetin are agonists of the aryl hydrocarbon receptor that differentially affect cytochrome P450 1A1 activity. *Cancer Res.* **58**, 2754–2760 (1998).
- 92. Chua, M. S. et al. Role of Cyp1A1 in modulation of antitumor properties of the novel agent 2-(4-amino-3-methylphenyl) benzothiazole (DF 203, NSC 674495) in human breast cancer cells. *Cancer Res.* **60**, 5196–5203 (2000).
- 93. Brantley, E. et al. Fluorinated 2-(4-amino-3-methylphenyl)benzothiazoles induce CYP1A1 expression, become metabolized, and bind to macromolecules in sensitive human cancer cells. *Drug Metab. Dispos.* 32, 1392–1401. https://doi.org/10.1124/dmd.104.0 01057 (2004).
- 94. Bradshaw, T. D. & Westwell, A. D. The development of the antitumour benzothiazole prodrug, Phortress, as a clinical candidate. *Curr. Med. Chem.* 11, 1009–1021. https://doi.org/10.2174/0929867043455530 (2004).
- 95. Trapani, V. et al. DNA damage and cell cycle arrest induced by 2-(4-amino-3-methylphenyl)-5-fluorobenzothiazole (5F 203, NSC 703786) is attenuated in aryl hydrocarbon receptor deficient MCF-7 cells. *Br. J. Cancer.* 88, 599–605. https://doi.org/10.1038/sj.bjc.6600722 (2003).

- 96. Loaiza-Perez, A. I. et al. Aryl hydrocarbon receptor activation of an antitumor aminoflavone: basis of selective toxicity for MCF-7 breast tumor cells. *Mol. Cancer Ther.* **3**, 715–725 (2004).
- 97. Meng, L. H. et al. Activation of aminoflavone (NSC 686288) by a sulfotransferase is required for the antiproliferative effect of the drug and for induction of histone gamma-H2AX. *Cancer Res.* 66, 9656–9664. https://doi.org/10.1158/0008-5472.CAN-06-0796 (2006).
- 98. Androutsopoulos, V., Arroo, R. R., Hall, J. F., Surichan, S. & Potter, G. A. Antiproliferative and cytostatic effects of the natural product eupatorin on MDA-MB-468 human breast cancer cells due to CYP1-mediated metabolism. *Breast Cancer Res.* 10, R39. https://doi.org/10.1186/bcr2090 (2008).
- 99. Androutsopoulos, V., Wilsher, N., Arroo, R. R. & Potter, G. A. Bioactivation of the phytoestrogen diosmetin by CYP1 cytochromes P450. Cancer Lett. 274, 54–60. https://doi.org/10.1016/j.canlet.2008.08.032 (2009).
- 100. Androutsopoulos, V. P., Mahale, S., Arroo, R. R. & Potter, G. Anticancer effects of the flavonoid diosmetin on cell cycle progression and proliferation of MDA-MB 468 breast cancer cells due to CYP1 activation. *Oncol. Rep.* 21, 1525–1528. https://doi.org/10.3892/ or 00000384 (2009).
- 101. Fang, M. et al. Effect-directed analysis of Elizabeth River porewater: Developmental toxicity in zebrafish (Danio rerio). Environ. Toxicol. Chem. 33, 2767–2774. https://doi.org/10.1002/etc.2738 (2014).
- 102. Powell, W. H. et al. Cloning and analysis of the CYP1A promoter from the atlantic killifish (Fundulus heteroclitus). *Mar. Environ. Res.* **58**, 119–124. https://doi.org/10.1016/j.marenvres.2004.03.005 (2004).
- 103. Jantzen, H. M. et al. Cooperativity of glucocorticoid response elements located far upstream of the tyrosine aminotransferase gene. *Cell* 49, 29–38. https://doi.org/10.1016/0092-8674(87)90752-5 (1987).
- 104. Dynan, W. S. & Tjian, R. The promoter-specific transcription factor Sp1 binds to upstream sequences in the SV40 early promoter. *Cell* 35, 79–87. https://doi.org/10.1016/0092-8674(83)90210-6 (1983).
- 105. Segal, J. A., Barnett, J. L. & Crawford, D. L. Functional analyses of natural variation in Sp1 binding sites of a TATA-less promoter. J. Mol. Evol. 49, 736–749. https://doi.org/10.1007/pl00006596 (1999).
- 106. Zeruth, G. & Pollenz, R. S. Functional analysis of cis-regulatory regions within the dioxin-inducible CYP1A promoter/enhancer region from zebrafish (Danio rerio). *Chem. Biol. Interact.* **170**, 100–113. https://doi.org/10.1016/j.cbi.2007.07.003 (2007).
- 107. Montminy, M. R., Sevarino, K. A., Wagner, J. A., Mandel, G. & Goodman, R. H. Identification of a cyclic-AMP-responsive element within the rat somatostatin gene. *Proc. Natl. Acad. Sci. U S A.* 83, 6682–6686. https://doi.org/10.1073/pnas.83.18.6682 (1986).
- 108. Gronostajski, R. M., Adhya, S., Nagata, K., Guggenheimer, R. A. & Hurwitz, J. Site-specific DNA binding of nuclear factor I: analyses of cellular binding sites. *Mol. Cell. Biol.* 5, 964–971. https://doi.org/10.1128/mcb.5.5.964-971.1985 (1985).
- 109. Yanagida, A., Sogawa, K., Yasumoto, K. I. & Fujii-Kuriyama, Y. A novel cis-acting DNA element required for a high level of inducible expression of the rat P-450c gene. Mol. Cell. Biol. 10, 1470–1475. https://doi.org/10.1128/mcb.10.4.1470-1475.1990 (1990)
- 110. Feingold, A. Effect sizes for growth-modeling analysis for controlled clinical trials in the same metric as for classical analysis. *Psychol. Methods.* **14**, 43–53. https://doi.org/10.1037/a0014699 (2009).

#### Acknowledgements

The authors thank Drs. R. Stephen Lloyd and Mitchell Turker for critical review of the manuscript.

#### **Author contributions**

C.W. and N.J. designed the experiments, in consultation with R.T.D., J.N.M, and R.T. R.T. and N.J. caught wild fish and performed breeding and exposure experiments. N.P. and S.C. performed *CYP1A* resequencing. S.C. and E.W. performed gene expression experiments. S.C. performed ChIP experiments. The OHSU Biostatistical Design Program staff performed statistical analyses. C.W. wrote the manuscript and all co-authors reviewed and edited the manuscript. C.W. oversaw the project.

#### **Declarations**

#### Competing interests

The authors declare no competing interests.

#### Additional information

**Supplementary Information** The online version contains supplementary material available at https://doi.org/1 0.1038/s41598-024-82740-w.

Correspondence and requests for materials should be addressed to C.W.

Reprints and permissions information is available at www.nature.com/reprints.

**Publisher's note** Springer Nature remains neutral with regard to jurisdictional claims in published maps and institutional affiliations.

**Open Access** This article is licensed under a Creative Commons Attribution-NonCommercial-NoDerivatives 4.0 International License, which permits any non-commercial use, sharing, distribution and reproduction in any medium or format, as long as you give appropriate credit to the original author(s) and the source, provide a link to the Creative Commons licence, and indicate if you modified the licensed material. You do not have permission under this licence to share adapted material derived from this article or parts of it. The images or other third party material in this article are included in the article's Creative Commons licence, unless indicated otherwise in a credit line to the material. If material is not included in the article's Creative Commons licence and your intended use is not permitted by statutory regulation or exceeds the permitted use, you will need to obtain permission directly from the copyright holder. To view a copy of this licence, visit <a href="https://creativecommons.org/licenses/by-nc-nd/4.0/">https://creativecommons.org/licenses/by-nc-nd/4.0/</a>.

© The Author(s) 2025